R-05-22

Rock mechanics site descriptive model– theoretical approach

Preliminary site description Forsmark area – version 1.2

Anders Fredriksson, Isabelle Olofsson
Golder Associates AB

December 2005

Svensk Kärnbränslehantering AB
Swedish Nuclear Fuel
and Waste Management Co
Box 5864
SE-102 40 Stockholm Sweden
Tel 08-459 84 00
+46 8 459 84 00
Fax 08-661 57 19
+46 8 661 57 19

ISSN 1402-3091
SKB Rapport R-05-22

Rock mechanics site descriptive model – theoretical approach

Preliminary site description Forsmark area – version 1.2

Anders Fredriksson, Isabelle Olofsson
Golder Associates AB

December 2005

Abstract

The present report summarises the theoretical approach to estimate the mechanical properties of the rock mass in relation to the Preliminary Site Descriptive Modelling, version 1.2 Forsmark.

The theoretical approach is based on a discrete fracture network (DFN) description of the fracture system in the rock mass and on the results of mechanical testing of intact rock and on rock fractures.

To estimate the mechanical properties of the rock mass a load test on a rock block with fractures is simulated with the numerical code 3DEC. The location and size of the fractures are given by DFN-realisations. The rock block was loaded in plain strain condition. From the calculated relationship between stresses and deformations the mechanical properties of the rock mass were determined.

The influence of the geometrical properties of the fracture system on the mechanical properties of the rock mass was analysed by loading 20 blocks based on different DFN-realisations. The material properties of the intact rock and the fractures were kept constant. The properties are set equal to the mean value of each measured material property.

The influence of the variation of the properties of the intact rock and variation of the mechanical properties of the fractures are estimated by analysing numerical load tests on one specific block (one DFN-realisation) with combinations of properties for intact rock and fractures. Each parameter varies from its lowest values to its highest values while the rest of the parameters are held constant, equal to the mean value. The resulting distribution was expressed as a variation around the value determined with mean values on all parameters.

To estimate the resulting distribution of the mechanical properties of the rock mass a Monte-Carlo simulation was performed by generating values from the two distributions independent of each other. The two values were added and the statistical properties of the resulting distribution were determined.

Sammanfattning

Denna rapport sammanfattar det teoretiska angreppssättet att uppskatta bergmassans mekaniska egenskaper i samband med den Platsbeskrivande modellen version 1.2 för Forsmark.

Det teoretiska angreppssättet baseras dels på en geometrisk DFN-beskrivning av bergmassans spricksystem och dels mekaniska laboratorietester utförda på intakt berg och på bergsprickor.

För att uppskatta bergmassans mekaniska egenskaper utförs ett numeriskt belastningsförsök på ett bergblock i den numeriska koden 3DEC. Läge och storlek på sprickorna i blocket baseras på DFN-realiseringar. Blocket belastas under plant töjningstillstånd.

Inverkan av spricksystemets geometriska utformning bestäms genom att analysera cirka 20 stycken DFN-realiseringar med konstanta egenskaper hos det intakta berget och hos sprickorna. Egenskaperna har satts lika med de uppmätta medelvärdena för respektive egenskap.

Inverkan av det intakta bergets och sprickornas mekaniska egenskaper bestäms genom att för en DFN-realisering utföra analyser med kombinationer av egenskaper. Varje parameter varieras mellan dess lägsta och högsta värde medan övriga parametrar hålls konstanta. Den resulterande fördelningen uttrycks som variation kring det värde som bestämts med medelvärde på alla egenskaper.

För att erhålla den resulterande fördelningen på bergmassans egenskaper görs Monte-Carlo-simuleringar där ett värde slumpas fram ur de bestämda fördelningarna över spricksystemets geometriska inverkan och inverkan av variation av delkomponenternas egenskaper. De två värdena adderas för att erhålla den resulterande fördelningen hos bergmassans mekaniska egenskaper.

Symbols and abbreviations

c_i	Cohesion of intact rock (MPa)
c_f	Peak cohesion of fracture (MPa)
c_m	Cohesion of rock mass (MPa)
D	Density (kg/m^3)
epsh	Horizontal strain
epsv	Vertical strain
epsx	Strain in the X direction (horizontal)
epsy	Strain in the Y direction (vertical)
epsz	Strain in the Z direction
E_i	Young's modulus of the intact rock (GPa)
E_m	Young's modulus of the rock mass (GPa)
K_n	Joint normal stiffness at expected normal stress (MPa/m)
K_s	Joint shear stiffness at expected normal stress (MPa/m)
k_r	Exponent in Power Law size distribution
jr	Material parameter for joint roughness (m)
$\Delta\sigma_y$	Increment in stress along y-axis (MPa)
ε_x	Strain in the X direction (horizontal)
ε_y	Strain in the Y direction (vertical)
ϕ_f	Internal friction angle of fractures (°)
ϕ_i	Internal friction angle of intact rock (°)
ϕ_m	Internal friction angle of rock mass (°)
ν_i	Poisson's ratio of the intact rock
ν_m	Poisson's ratio of the rock mass
σ_1	Maximum stress (MPa)
σ_2	Intermediate stress (MPa)
σ_3	Minimum stress (MPa)
σ_h	Intermediate horizontal in situ stress (MPa)
σ_H	Maximum horizontal in situ stress (MPa)
σ_v	Vertical stress (MPa)
σ_{vf}	Vertical sterss at failure (MPa)
σ_{vmax}	Maximal vertical stress (MPa)
T_i	Tensile strength of intact rock(MPa)
UCS_i	Uniaxial compressive strength of intact rock (MPa)
UCS_m	Uniaxial compressive strength of rock mass (MPa)
X_{r0}	Minimum radius in Power Law size distribution (m)

Contents

1 Introduction

This work reports results from one of the four rock mechanics activities that have been recognised within the project "Forsmark – Site Descriptive Model during the initial Site Investigation stage version 1.2". This activity aims to determine the undisturbed mechanical properties of the rock mass in the local model area for Forsmark 1.2. These parameters will be distributed to the "Design team" which will evaluate the suitability of the site.

One approach used in this activity is based on numerical simulations with the use of the 3DEC software. The methodology has been developed in the purpose of the Site Investigations and is built upon three different models: the DFN model which is used to simulate the fracture network in the rock mass, the 3DEC mechanical model which is used to calculate the rock mass mechanical properties, and the GoldSim model which is the tool for estimation of combined variabilities.

The modelling procedure is described in detail in /Olofsson and Fredriksson, 2005/.

The work was conducted according to the Activity Plan for "Establishment of a Rock Mechanics model for Forsmark 1.2".

The DFN model, the in situ stresses as well as the mechanical properties of intact rock and fractures constitute the input data that are necessary to build the 3DEC model. Then the set-up of the 3DEC model and the procedure used for numerical simulations are described. The results obtained from simulations in 3DEC and GoldSim are reviewed and analysed, and the summary tables of mechanical properties of the rock mass are presented.

2 Indata

2.1 Intact rock

/Lanaro and Fredriksson, 2005/ described the mechanical properties for the intact rock and these are summarised in Table 2-1.

Table 2-2 presents the lithological description of the rock domain RFM029, which was required to know what parameters of the intact rock need to be inserted in the numerical model. One rock type, granite to granodiorite, is strongly dominant, and the intact rock parameters for this rock type were used for numerical modelling.

The truncated normal distributions as given in Table 2-1 are illustrated in Figure 2-1 for cohesion and in Figure 2-2 for friction angle for the granite to granodiorite. The relationship between σ_1 and σ_3 is illustrated in Figure 2-3 for the same rock type.

Table 2-1. Predicted rock mechanical properties for intact rock (matrix) for two rock types (i.e. small pieces of rock without any fractures).

Parameter for intact rock (drill core scale)	Granite to granodiorite Truncated normal distribution Mean/standard dev	Granite to granodiorite Min trunc – Max trunc	Tonalite Truncated normal distribution Mean/standard dev	Tonalite Min trunc – Max trunc
Uniaxial compressive strength, UCS_i	225 (MPa) / 22 (MPa)	182 – 269 (MPa)	156 (MPa) / 13 (MPa)	132 – 181 (MPa)
Young's modulus, E_i	76 (GPa) / 3 (GPa)	71 – 81 (GPa)	72 (GPa) / 3 (GPa)	66 – 79 (GPa)
Poisson's ratio, ν_i	0.24 / 0.04	0.17 – 0.31	0.27 / 0.04	0.20 – 0.34
Tensile strength, T_i	13.3 (MPa) / 1.8 (MPa)	10 – 17 (MPa)	15.2 (MPa) / 1.2 (MPa)	13 – 18 (MPa)
Mohr – Coulomb, ϕ_i	60.0 (°) / 0.4 (°)	59.2 (°) – 60.6 (°)	47.0 (°) / 1.6 (°)	43.4 (°) – 49.8 (°)
Mohr – Coulomb, c_i	30.2 (MPa) / 2.6 (MPa)	23.9 – 37 (MPa)	30.8 (MPa) / 2.5 (MPa)	24.8 – 37.7 (MPa)

/Lanaro and Fredriksson, 2005/ gave the correlation between Ø and c as –0.2306 for granite to granodiorite and –0.4478 for tonalite.

Table 2-2. Rock types in the simulated rock domain RFM029.

	Main rock type	%	Subordinate rock types	%
RFM029	Granite to granodiorite, metamorphic	84	Granitoid, metamorphic	10
			Amphibolite	3
			Pegmatite, pegmatitic granite	2
			Granite, fine to medium-grained	1

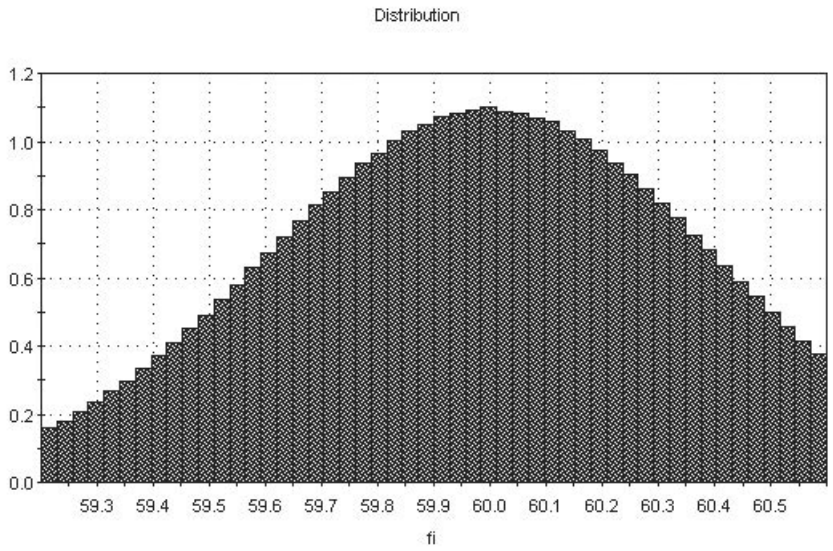

Figure 2-1. *Truncated normal distribution of ϕ. Granite to granodiorite.*

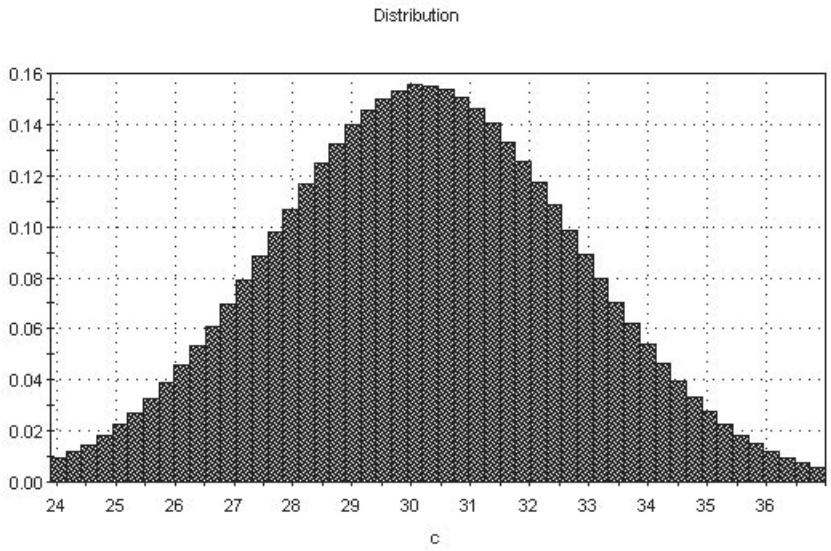

Figure 2-2. *Truncated normal distribution of c. Granite to granodiorite.*

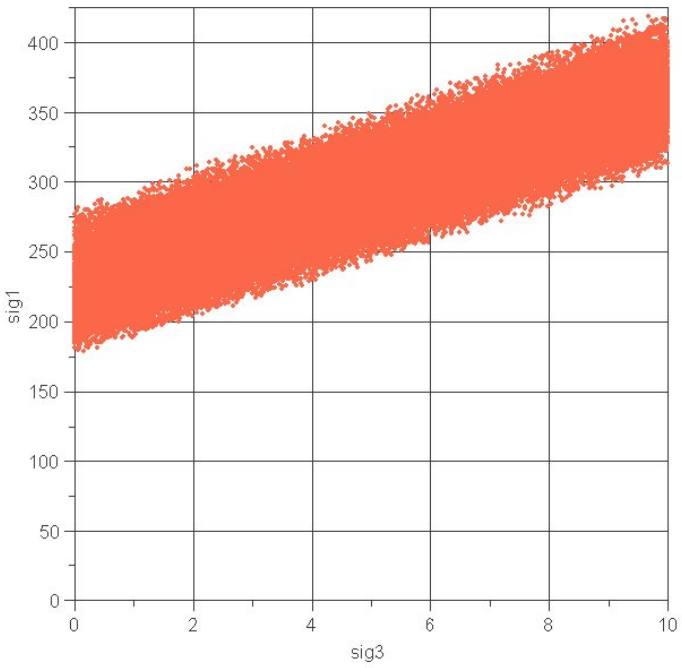

Figure 2-3. *Relationship between σ_1 and σ_3 at failure. Granite to granodiorite.*

2.2 Fractures

2.2.1 Geometry of fractures

The parameters for the DFN model were delivered and presented first on the 20 September 2004. The model was not the final version but regarding the time schedule for the Rock Mechanics model, statistical parameters given during this meeting were used for most of the simulations.

The final DFN model was delivered with two alternatives for the same conceptual models for intensity of fractures. Some simulations could be run with this model mostly to determine the influence of the change of fracture intensity on the rock mass mechanical parameters.

An updated version of the DFN model was presented in March 2005. For this model some analyzes were performed to see that the changes in the DFN model do not influence the rock mass properties too much.

The DFN model was developed for orientation and fracture size based on 4 sub-vertical sets of fractures and one sub-horizontal set of fractures. The 4 sub-vertical sets (NS, NE, NW and EW) are defined as regional and lineament-related sets and their characterisation (orientation and size distribution) is based on information from outcrops and lineaments. Sub-horizontal fractures (SubH) are also considered to belong to the background fracturing of the rock mass but their characterisation is mostly based on borehole data.

The two alternatives to the DFN conceptual model were based on borehole fracture intensity and result from the way simulations for estimating the volumetric fracture intensity in the rock mass were carried /LaPointe et al. 2005/.

The parameters for the DFN model have been studied and used for simulating the 3D fracture network required for setting-up the numerical mechanical model. These are presented below.

Orientation

The mean trend and plunge and dispersion are given for each set, disregarding the fractures being open, partly open or closed (definition according to BOREMAP mapping), see Table 2-3. The mean axis trend and plunge that are required for generating bivariate distributions are given in Table 2-4.

Table 2-3. Orientation of all fracture sets.

Set	Best model	Mean pole trend	Mean pole plunge	Dispersion	Other acceptable models
NS	Bivariate Fisher	92.4	5.9	k1=19.31, k2=19.69	None
NE	Bivariate Bingham	137.3	3.7	k1=–17.09, k2=–9.1	Bivariate Fisher at 2.2%
NW	Fisher	40.6	2.2	k=23.9	None
EW	Fisher	190.4	0.7	k=30.63	None
SubH	Fisher	342.9	80.3	k=8.18	All others

Table 2-4. Major axis trend and plunge of the fracture sets.

Set	Major axis trend	Minor axis trend
NS	355.3	50.2
NE	38.1	68.2
NW	220.6	87.8
EW	10.4	89.3
SubH	162.9	9.7

Size distribution

The size distribution used is the one provided in the DFN model version 1.2 and the parameters of the power law distribution are given in Table 2-5. For numerical reasons in 3DEC only fractures with a radius bigger than 1 m were generated.

Table 2-5. Size distribution for all fracture sets.

Set	Size model	Powerlaw (Parent radius distribution)		
		Upper k_r / X_{r0}	Median k_r / X_{r0}	Lower k_r / X_{r0}
NS	Power law	2.94/0.421	2.88/0.315	2.78/0.326
NE	Power law	3.05/0.085	3.02/0.083	2.94/0.084
NW	Power law	2.87/0.644	2.81/0.374	2.71/0.178
EW	Power law	3.03/0.465	2.95/0.341	2.77/0.879
SubH	Power law	3.02/0.5	2.92/0.633	2.97/0.863

Intensity

The concept of the model for intensity that is used for the rock mechanics model is based on fracture frequency data from boreholes. Two alternatives were developed which are related to different approaches for the simulations and calculations of P_{32} from P_{10} data /LaPointe et al. 2005/.

For the purpose of the Rock Mechanics model, the DFN model was simulated only in the rock domain 29. Table 2-6 presents the P_{32} values for the first alternative and Table 2-7 gives the P_{32} values for the second alternative.

Table 2-6. Alternative 1: P_{32} for all fracture sets in the rock domain 29 (RFM029).

Set	P_{32} open[1], mean	P_{32} sealed, mean	P_{32} open[1], std deviation	P_{32} sealed, std deviation
NS	0.132	0.47	0.269	0.275
NE	0.508	1.561	1.041	0.915
NW	0.177	0.271	0.364	0.159
EW	0.057	0.169	0.117	0.099
SubH	0.346	0.259	0.729	0.152

[1] Open inclusive partly open.

Table 2-7. Alternative 2: P_{32} for all fracture sets in the rock domain 29 (RFM029).

Set	P_{32} open[1], mean	P_{32} sealed, mean	P_{32} open[1], std deviation	P_{32} sealed, std deviation
NS	0.044	0.245	0.083	0.153
NE0	0.17	0.813	0.028	0.509
NW	0.19	0.141	0.008	0.088
EW	0.058	0.088	0.003	0.055
SubH	0.110	0.135	0.006	0.085

[1] Open inclusive partly open.

2.2.2 Mechanical properties of fractures

Laboratory normal load tests up to 10 MPa and shear tests have been performed on fractures at normal stress levels of 0.5, 5 and 20 MPa from borehole KFM01A, KFM02A, KFM03A and KFM04A. The laboratory tests were evaluated and the results given by /Lanaro and Fredriksson, 2005/.

The data was statistically analysed and a truncated normal distribution was assumed to be a reasonable approximation to the data. The preliminary mechanical properties of fractures that are to be used at this stage are presented in Table 2-8 in terms of mean, span and range of potential values for each parameter.

Table 2-8. Summary of mechanical properties of fractures evaluated from laboratory tests.

Parameter for single fractures (small scale)	All fracture sets Truncated normal distribution Mean/Standard deviation	Min trunc – Max trunc
Normal stiffness, K_n	128.4 / 51.6 (MPa/mm)	68.0 – 288.4 (MPa/mm)
Shear stiffness, K_s	38.8 / 10.8 (MPa/mm)	11.2 – 55.1 (MPa/mm)
Peak friction angle, ϕ_f	34.0 (°) / 2.8 (°)	27.3 (°) – 39.1 (°)
Cohesion, c_f	0.6 / 0.3 (MPa)	0.0 / 1.1 (MPa)

The correlation between the peak friction angle, ϕ_f, and cohesion, c_f, are –0.1834.

2.3 In situ stresses

The in situ stress conditions were presented in /Lanaro and Fredriksson, 2005/. Table 2-9 shows the magnitude and orientation of in situ stresses predicted at 500 m depth.

Table 2-9. In situ stress conditions at 500 m depth.

	σ_1 (σ_H)	σ_2 (σ_h)	σ_3 (σ_v)
Magnitude (MPa)	45	30.5	13.5
Trend (°)	105	15	
Plunge	10	10	

3 Set-up of the model

3.1 Description of the numerical simulations

The parameters presented in Section 2.2.1 were used to generate the 3D fracture network used for extraction of fracture data into 3DEC.

The fracture networks were generated for rock domain RFM029. Twenty realisations of the same fracture network (i.e. with all input parameters equivalent) were simulated for the "base case". Only open and partly open fractures fractures were generated in the DFN model. Based on the results of laboratory tests, the assumption was made that sealed fractures do not significantly influence the mechanical behaviour of the rock mass.

When the 3D fracture networks were generated 2D vertical sampling planes parallel to the maximum and minimum stresses (σ_1 and σ_2) are extracted. The trace data on these planes were used for input in 3DEC. The identification of each fracture set was maintained throughout the process to allow different mechanical properties to be assigned to the different fracture sets.

Figure 3-1 gives an example of the generated fracture traces in a vertical plane. Figure 3-2 shows the corresponding 3DEC model. Each fracture in the 3DEC model is divided in a number of contact points. Each contact point correspond to an area of the fracture depending on the zone size given. In Figure 3-3 the contact points along each fracture in the 3DEC model are shown.

The result in the form of vertical stress-vertical strain and horizontal strain-vertical strain curves from one simulation with 3DEC is shown in Figure 3-4.

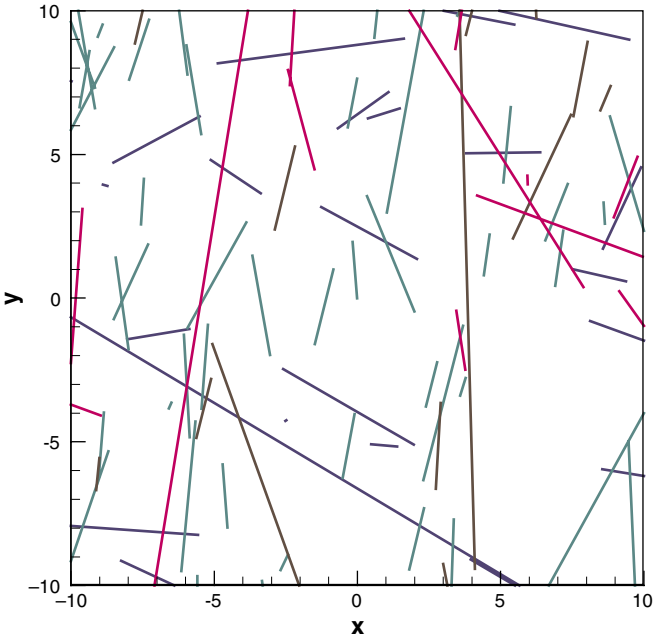

Figure 3-1. *Example of fracture traces in a vertical plan. Fracture traces from different fracture sets have different colours.*

Figure 3-2. *3DEC model generated from the fracture traces shown in Figure 3-1.*

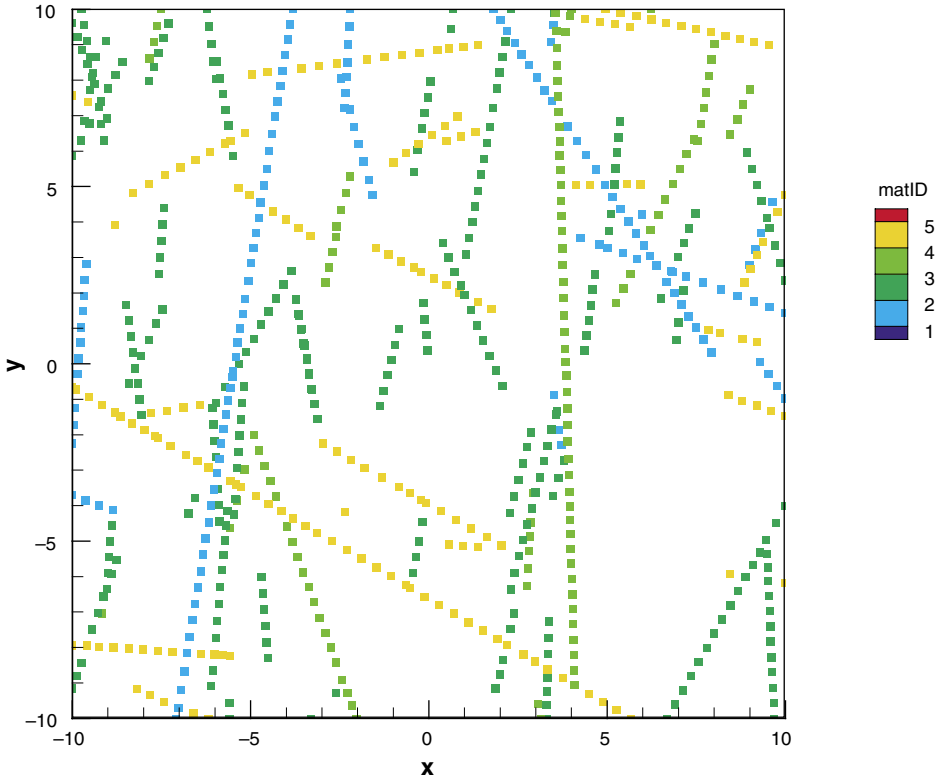

Figure 3-3. *Contact points along fractures in the 3DEC model.*

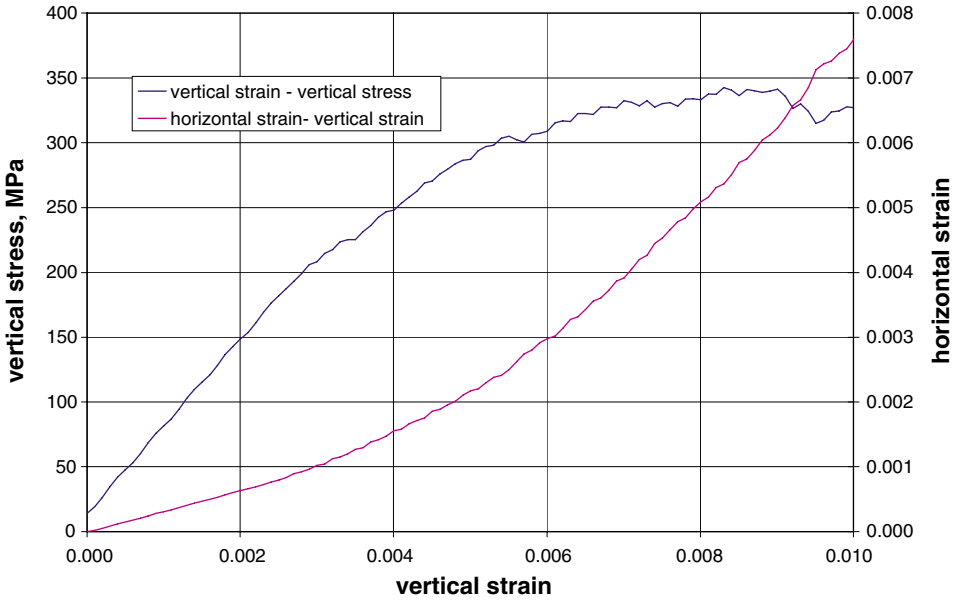

Figure 3-4. *Example of stress-strain curves.*

The deformation modulus, E_m, and Poisson's ratio, ν_m, of the rock mass were evaluated from stress-vertical strain and horizontal strain-vertical strain curves. The strength parameters of the rock mass, uniaxial strength, UCS_m, cohesion, c_m, and friction, ϕ_m, were evaluated from simulations with different confining stress. The following equations were used:

$$\phi_m = \arcsin(k-1 \,/\, k+1) \tag{3-1}$$

$$UCS_m = \sigma_{1b} + k \cdot \sigma_{3b} \tag{3-2}$$

$$c_m = UCS_m \cdot (1-\sin\phi_m) \,/\, 2 \cdot \cos\phi_m \tag{3-3}$$

where $k = (\sigma_{1a} - \sigma_{1b}) \,/\, (\sigma_{3a} - \sigma_{3b})$ and σ_{1a}, σ_{1b}, σ_{3a} and σ_{3b} are the principal stresses at failure at two confining stresses a and b.

Distributions of the four rock mass parameters (E_m, ν_m, c_m, and ϕ_m) are estimated at a block scale of 20 m, using the software 3DEC for the rock mechanical modeling part and GoldSim for subsequent Monte-Carlo simulations.

The procedure is described in more detail in /Olofsson and Fredriksson, 2005/.

The uncertainty of a model can be separated into conceptual uncertainty, data uncertainty and spatial variability. The conceptual uncertainty originates from an incomplete understanding of the principal structure of the analyzed system and its interacting processes. This uncertainty is not further discussed.

Data uncertainty concerns the uncertainty in parameter values being used in a model; it may be caused by measuring errors, interpretation errors or uncertainty in extrapolation of spatially variable parameters.

Spatial variability concerns the variation in space of a parameter value; although this is not strictly an uncertainty, in combination with practical limitations in rock characterization, it constitutes an indirect source for data uncertainty. Hence, in the following, no distinction is made to what extent the estimated rock mass parameter distributions relate to spatial variability and/or data uncertainty.

In the case of the present data, stochastic material properties of intact rock and of fractures are approximated by empirical, truncated, normal distributions that are defined by their mean, standard deviation, minimum and maximum values (Table 3-1). Likewise, the DFN geometry is given as stochastic distributions.

Ideally, rock mass property distributions could be estimated by iterative 3DEC simulations involving numerous stochastic DFN realizations, where the DFN geometry and material property parameters are allowed to take on any value from their defined input distributions. However, such a direct approach becomes impractical due to its computational demand and limitations in parameter descriptions in 3DEC.

Instead, a simpler stochastic approach is used. Here, 3DEC was only used to estimate the DFN geometry-induced variability and the influence input material parameters (intact rock and fractures) have on rock mass properties. The combined effect of DFN geometry-induced variability and the material property-induced variability was estimated by Monte-Carlo simulations using a simple GoldSim model.

The procedure for management of uncertainty is described in the methodology report /Olofsson and Fredriksson, 2005/.

3.2 Assumptions

The key concept used here is that the rock mass variability depending on the geometry of the fracture network (DFN-model) can be evaluated independently of the variability from the variation of mechanical properties of the fractures and the intact rock i.e. the rock properties are independent of one another. The variability can be evaluated separately and the total variability can be estimated by superimposing the effects of the two components.

Samples containing sealed fractures are treated as “intact rock” samples.

3.2.1 Input material data

Statistical distributions of input parameters are shown in Table 3-1.

Table 3-1. Input parameter distributions for intact rock and fracture properties.

		Mean	Standard deviation	Min	Max
Intact rock, RFM029	E_i (GPa)	76	3	71	81
	ν_i (–)	0.24	0.04	0.17	0.31
	ϕ_i (°)	60	0.4	59.2	60.6
	c_i (MPa)	30.2	2.6	23.9	37
	T_i (MPa)	13.3	1.8	10	17
Fractures	K_n (MPa/mm)	128.4	51.6	68	288.4
	K_s (MPa/mm)	38.8	10.8	11.2	55.1
	ϕ_f (°)	34	2.8	27.3	39.1
	c_f (MPa)	0.6	0.3	0.0	1.1

3.2.2 Base for simulations

The distributions of rock mass properties estimated for this report (E_m, ν_m, c_m, and ϕ_m) were assumed to consist of two main components: (1) an intrinsic variability component caused by its stochastic DFN geometry and (2) a component induced by stochastic material properties of fractures (K_n, K_s, ϕ_f, and c_f) and those of intact rock (E_i, ν_i, ϕ_i, c_i, and T_i). Further, these two components are assumed to be independent, such that the total rock mass property distributions can be estimated by superimposing the DFN geometry-based and the material property-related variability components. The outline can be summarized as follows:

1. The variability component caused by stochastic fracture network geometry is evaluated for multiple DFN realisations; these were all assigned mean material-property values.
2. The influence that each individual material property has on the rock mass properties was estimated for one specific “average” realisation; it was done by examining the effect on rock mass parameters as each material property is assigned its minimum and maximum parameter values, while all other material properties were set to their mean values.
3. Next, based on the relationships obtained in step 2 combinations of input parameters were tested to get the span of the material property variability. The statistical distributions of the influence of material properties on rock mass parameters were calculated.
4. Finally, the DFN geometry-induced and the material property-related components were superimposed to estimate the total ranges of rock mass parameter distributions.

4 Simulations on the alternative 1 of DFN model

4.1 Simulations parallel to σ_1

The mechanical model was first tested for trace planes parallel to the maximal principal stress.

4.1.1 DFN geometry-induced rock mass variability

These simulations were run in order to quantify the influence of the fracture pattern on the rock mass mechanical parameters. This is achieved by running 21 realisations of the same DFN model (Monte-Carlo simulations) in 3DEC while the input mechanical parameters remain constant. Calculated stress-strain curves are shown in Figure 4-1. The statistical parameters used for simulating the DFN model are listed in Table 2-3 to Table 2-6.

21 simulations of the DFN model were analysed at two different stress levels, 45 MPa (equivalent to the maximum principal stress) and 11.3 MPa (25% of σ_1). The mechanical models were loaded with a constant velocity in the vertical direction while the horizontal stresses were constant during the loading test. The deformation modulus, E_m, Poisson's ratio, ν_m, and the vertical stress at failure, σ_{vf}, were evaluated at both stress levels to provide an estimation of ϕ_m and c_m. The stress at failure, σ_{vf}, is defined as the maximum vertical stress or the vertical stress at 0.010 vertical strain if the vertical stress-vertical strain curve do not show a marked maximum.

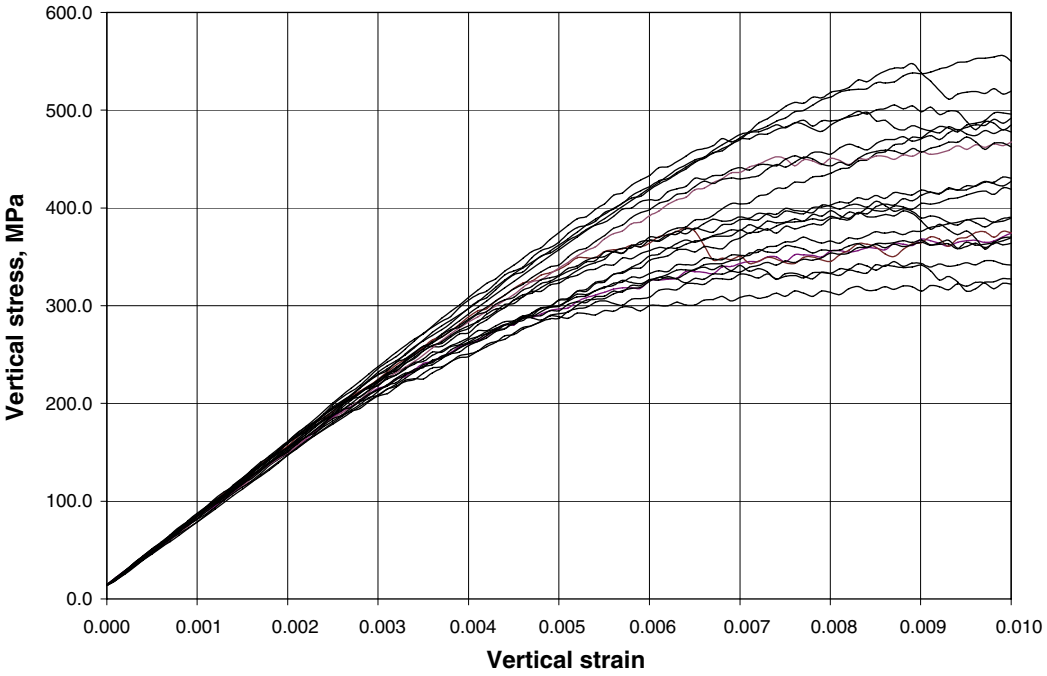

Figure 4-1. *Calculated stress-strain curves with 3DEC.*

The input properties used for the simulations are mean values of intact rock and mean values of fracture properties as given in Table 3-1.

The evaluated rock mass parameters, E_m and ν_m at 45 MPa and 11.3 MPa for each realisation are presented in Appendix A Tables A-1 and A-2.

The evaluated cohesion and friction angle of the rock mass for each realisation are presented in Appendix A Table A-3. These parameters were evaluated by fitting a straight line between the vertical stress at failure at both stress levels. The uniaxial compressive strength of the rock mass has been calculated from the evaluated cohesion and friction angle.

A summary of the obtained distributions for $E_{m\ 45\ Mpa}$, $\nu_{m\ 45\ MPa}$, $E_{m\ 11.3\ MPa}$, $\nu_{m\ 11.3\ MPa}$, ϕ_m and c_m are summarized in Table 4-1 for Rock Domain RFM029. The parameters that are given in this table only account for the influence of the variation in the fracture pattern on the rock mass properties (as input mechanical parameters are constant).

Table 4-1. DFN geometry-induced variability in rock mass properties of Rock Domain RFM029.

	Mean	Standard deviation	Min	Max
$E_{m\ 45\ Mpa}$ (GPa)	66.0	2.4	62.1	70.0
$\nu_{m\ 45\ MPa}$	0.24	0.005	0.23	0.25
$E_{m\ 11.3\ MPa}$ (GPa)	64.9	3.4	57.5	70.3
$\nu_{m\ 11.3\ MPa}$	0.24	0.01	0.23	0.27
ϕ_m (°)	48.4	3.1	42.6	53.7
c_m (MPa)	21.0	4.8	13.8	28.6

The correlation between the friction angle, ϕ_m, and cohesion, c_m, are 0.0489.

4.1.2 Material property influence on rock mass parameters

These simulations were run in order to assess the influence of the variation of material input parameters on the rock mass mechanical parameters. This was achieved by using always the same DFN realisation while the mechanical input parameters are changed one at a time and are attributed its minimum and maximum values while all other material properties are set to their mean values. Relationships were then established between variations in all input material parameters and their respective impact on rock mass properties.

The same confining stresses as used in Section 4.1.1 were applied on the model: 45 MPa and 11.3 MPa.

Table 4-2 presents the effect of variation for each of the input parameters on the rock mass parameters when the input parameter is given its minimum value. A positive value indicates that the rock mass mechanical parameter increases when the input parameter decreases from its mean to its minimum value.

Table 4-3 illustrates the influence of input parameters at their maximum value.

Table 4-4 presents the calculated influence on rock mass deformation modulus of 2 extreme combinations that are expected to give respectively the highest and lowest deformation modulus. The estimated influence is given in relation to the deformation modulus obtained for input parameters at their mean value.

Table 4-2. Influence on the rock mass mechanical properties of the input mechanical parameters set at their min value (H is for the high stress level, L for the low stress level).

	E_{mH} (GPa)	ν_{mH}	E_{mL} (GPa)	ν_{mL}	ϕ_m (°)	c_m (MPa)
E_i (GPa)	–3.46	0.00	–0.51	–0.02	–0.45	2.11
ν_i	0.12	0.06	3.12	–0.08	0.74	–1.66
ϕ_i (°)	0.01	0.00	2.65	–0.01	–0.65	1.06
c_i (MPa)	–0.01	0.00	2.64	–0.01	0.10	–2.66
T_i (MPa)	0.00	0.00	2.66	–0.01	0.26	0.97
K_n (MPa/mm)	–1.98	0.01	5.80	–0.06	–1.18	3.51
K_s (MPa/mm)	–11.03	–0.01	–4.76	–0.01	1.19	–3.27
ϕ_f (°)	0.69	0.00	7.52	–0.04	–0.59	–3.64
c_f (MPa)	0.02	0.00	1.90	–0.01	–0.17	1.12

Table 4-3. Influence on the rock mass mechanical properties of the input mechanical parameters set at their max value (H is for the high stress level, L for the low stress level).

	E_{mH} (GPa)	ν_{mH}	E_{mL} (GPa)	ν_{mL}	ϕ_m (°)	c_m (MPa)
E_i (GPa)	3.40	0.00	5.94	–0.01	0.81	–2.09
ν_i	–0.36	0.04	2.66	0.04	–0.04	–0.57
ϕ_i (°)	0.02	0.00	2.66	–0.01	0.66	–1.62
c_i (MPa)	0.05	0.00	2.67	–0.01	–0.27	4.84
T_i (MPa)	0.01	0.00	2.66	–0.01	0.34	–1.67
K_n (MPa/mm)	1.57	0.00	9.53	–0.03	–0.09	–0.49
K_s (MPa/mm)	2.04	–0.02	9.74	–0.05	–1.01	3.15
ϕ_f (°)	0.06	–0.06	4.46	–0.03	2.14	1.87
c_f (MPa)	0.01	0.00	3.11	–0.02	–0.31	1.86

Table 4-4. Influence on the rock mass mechanical properties of the extreme combination of input mechanical parameters (H is for the high stress level, L for the low stress level).

	E_{mH} (GPa)	ν_{mH}	E_{mL}(GPa)	ν_{mL}	ϕ_m (°)	c_m,(MPa)
Comb 1	7.49	0.00	16.12	–0.03	–0.45	0.97
Comb 2	–13.93	0.01	–8.73	0.00	0.74	–2.74

Based on the calculated estimated influence of input parameter variation on the rock mass mechanical properties, specific combinations of input parameters with high and low values were chosen. These are expected to produce low and high deformation modulus or uniaxial compressive strength. 3DEC simulations were done with these combinations on DFN realisation nr 0. The results of these combinations are expressed in term of mean value, standard deviation, min and max values, and are presented in Table 4-5. The mean, min and max values are given in relation to the rock mass mechanical properties for the input parameters set at their mean value.

These simulations only account for the influence of the variation of input parameters on the rock mass mechanical properties.

Table 4-5. Influence on the rock mass properties of the combinations run in 3DEC (H is for the high stress level, L for the low stress level).

	E_{mH} (GPa)	ν_{mH}	E_{mL} (GPa)	ν_{mL}	ϕ_m (°)	c_m (MPa)
Mean	–0.73	0.01	3.42	–0.02	0.09	0.05
Standard dev	4.45	0.02	5.08	0.02	0.78	2.38
Min	–13.93	–0.06	–8.74	–0.08	–1.18	–3.64
Max	7.49	0.06	16.12	0.04	2.14	4.84

4.1.3 Monte-Carlo simulations

These were run to estimate the variability of the rock mass mechanical properties based on the estimated two distributions obtained in Sections 4.1.1 and 4.1.2:

1. One distribution which accounts only for the variation of the fracture pattern by means of 21 DFN realisations run in 3DEC.
2. One distribution which accounts for the variation of the input mechanical parameters in the 3DEC simulations. This distribution was obtained from 3DEC simulations on one DFN realisation. The influence of the variation of the input mechanical parameters is assumed to be similar for all DFN realisations.

In order to combine the effect of variation of fracture pattern and input mechanical parameters Monte-Carlo simulations were carried out in Goldsim. The procedure for simulations was the following:

- One random value was extracted from the distribution which describes the influence of the variation of the fracture pattern.
- A random value extracted from the distribution accounting for the variation of input mechanical parameters is added to the precedent value. This variation is related to the fracture pattern (according to Table 4-5).
- 100.000 random values are produced from both distributions and the resulting properties are statistically analysed. The rock mass mechanical properties and their variation are presented in Table 4-6. The distributions were truncated such as a unique value has 95% probability to be in the range of the given distribution.

Based on the distribution obtained for ϕ_m and c_m the rock mass uniaxial compressive strength, UCS, can be calculated. The distribution is given in Table 4-7 and illustrated in Figure 4-2. The correlation between ϕ_m and c_m is 0.043. The relation between σ_1 and σ_3 at failure is illustrated in Figure 4-3.

Table 4-6. Distribution of the rock mass mechanical properties (accounting for variation in fracture pattern and input parameters).

	E_{mH} (GPa)	ν_{mH}	E_{mL} (GPa)	ν_{mL}	ϕ_m (°)	c_m (MPa)
Mean	64.94	0.25	68.04	0.22	48.48	20.82
Standard dev	4.51	0.02	5.62	0.02	2.66	4.03
Min	56.10	0.21	57.02	0.18	43.27	12.92
Max	73.78	0.29	79.06	0.26	53.69	28.72

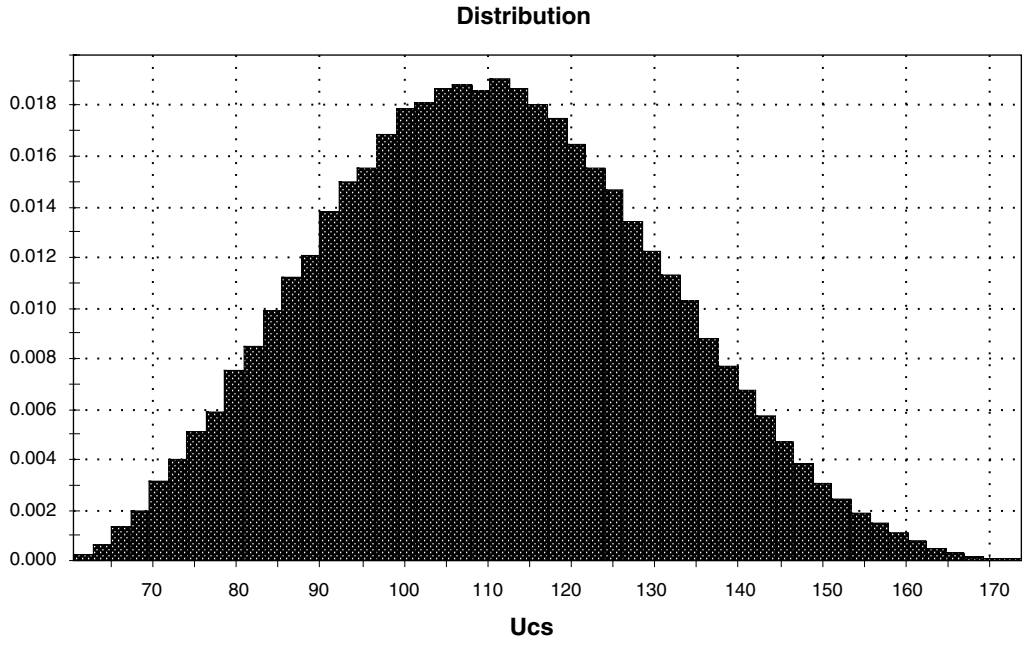

Figure 4-2. *UCS distribution.*

Table 4-7. Distribution of the rock mass UCS (accounting for variation in fracture pattern and input parameters).

	UCS_m (MPa)
Mean	110.31
Standard dev	19.70
Min	64.08
Max	165.43

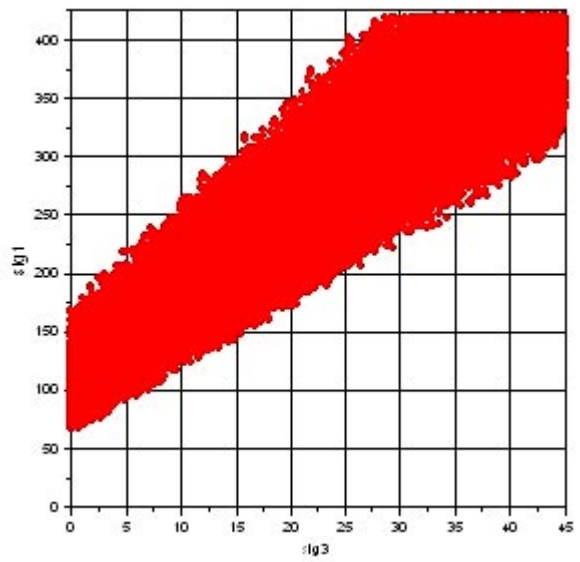

Figure 4-3. *Relation between σ_1 and σ_3 at failure.*

4.2 Simulations parallel to σ_2

The mechanical model was then tested for trace planes parallel to the minimal principal stress in the horizontal plane.

4.2.1 DFN geometry-induced rock mass variability

The procedure is exactly the same as described in Section 4.1.1.

The evaluated rock mass parameters, E_m and ν_m at 30.5 MPa and 8.0 MPa for each realisation are presented in Appendix B Tables B-1 and B-2.

The evaluated cohesion and friction angle of the rock mass for each realisation are presented in Appendix B Table B-3. These parameters were evaluated by fitting a straight line between the vertical stress at failure at both stress levels. The uniaxial compressive strength of the rock mass has been calculated from the evaluated cohesion and friction angle.

A summary of the obtained distributions for $E_{m\ 30.5\ Mpa}$, $\nu_{m\ 30.5\ MPa}$, $E_{m\ 8.0\ MPa}$, $\nu_{m\ 8.0\ MPa}$, ϕ_m and c_m are summarized in Table 4-8 for Rock Domain RFM029. The parameters that are given in this table only account for the influence of the variation in the fracture pattern on the rock mass properties (as input mechanical parameters are constant).

Table 4-8. DFN geometry-induced variability in rock mass properties of Rock Domain RFM029 parallel to σ_2.

	Mean	Standard deviation	Min	Max
$E_{m\ 30.5\ Mpa}$ (GPa)	66.4	2.3	61.7	70.1
$\nu_{m\ 30.5\ MPa}$	0.24	0.005	0.23	0.25
$E_{m\ 8.0\ MPa}$ (GPa)	63.4	4.4	51.1	68.8
$\nu_{m\ 8.0\ MPa}$	0.25	0.02	0.22	0.31
ϕ_m (°)	48.3	3.8	40.1	54.7
c_m (MPa)	18.8	7.5	10.2	40.5

The correlation between the friction angle, ϕ_m, and cohesion, c_m, are –0.44.

4.2.2 Material property influence on rock mass parameters

The procedure is exactly the same as the one described in Section 4.1.2.

Table 4-9 presents the effect of variation for each of the input parameters on the rock mass parameters when the input parameter is given its min value. A positive value indicates that the rock mass mechanical parameter increases when the input parameter decreases from its mean to its min value.

Table 4-10 illustrates the influence of input parameters at their maximum value.

Table 4-9. Influence on the rock mass mechanical properties of the input mechanical parameters set at their min value (H is for the high stress level, L for the low stress level).

	E_{mH} (GPa)	ν_{mH}	E_{mL} (GPa)	ν_{mL}	ϕ_m (°)	c_m (MPa)
E_i (GPa)	–4.14	0.00	–3.81	0.00	–0.98	2.23
ν_i	–0.86	–0.06	3.23	–0.05	–0.38	0.15
ϕ_i (°)	0.02	0.00	–0.02	0.00	–0.87	2.02
c_i (MPa)	0.01	0.00	0.07	0.00	0.08	–3.50
T_i (MPa)	0.02	0.00	–0.03	0.00	–0.33	1.71
K_n (MPa/mm)	–2.64	–0.02	–1.67	–0.01	0.72	–1.07
K_s (MPa/mm)	–4.84	0.02	–1.51	0.02	–0.71	2.05
ϕ_f (°)	–1.66	0.01	–0.85	0.02	–0.65	–1.34
c_f (MPa)	–0.03	0.00	–0.14	0.01	0.07	–0.04

Table 4-10. Influence on the rock mass mechanical properties of the input mechanical parameters set at their maximum value (H is for the high stress level, L for the low stress level).

	E_{mH} (GPa)	ν_{mH}	E_{mL} (GPa)	ν_{mL}	ϕ_m (°)	c_m (MPa)
E_i (GPa)	3.98	0.00	3.99	0.00	0.13	–0.03
ν_i	–1.13	0.06	3.23	–0.05	–0.20	1.06
ϕ_i (°)	0.01	0.00	0.03	0.00	–0.67	2.30
c_i (MPa)	0.05	0.00	–0.08	0.00	0.34	2.96
T_i (MPa)	0.00	0.00	0.04	0.00	–0.33	1.71
K_n (MPa/mm)	1.18	0.01	1.90	0.01	–0.07	–0.68
K_s (MPa/mm)	0.26	0.00	0.49	0.00	–1.34	4.12
ϕ_f (°)	0.20	0.00	1.47	–0.01	1.99	–2.18
c_f (MPa)	0.07	0.00	0.27	0.00	–0.49	1.40

Table 4-11 presents the calculated influence on rock mass deformation modulus of 2 extreme combinations that are expected to give respectively the highest and lowest deformation modulus. The estimated influence is given in relation to the deformation modulus obtained for input parameters at their mean value.

Based on the calculated estimated influence of input parameter variation on the rock mass mechanical properties, specific combinations of input parameters with high and low values were chosen. These are expected to produce low and high deformation modulus or uniaxial compressive strength. 3DEC simulations were done with these combinations on DFN realisation nr 1. The results of these combinations are expressed in term of mean value, standard deviation, min and max values, and are presented in Table 4-12. The mean, min and max values are given in relation to the rock mass mechanical properties for the input parameters set at their mean value.

These simulations only account for the influence of the variation of input parameters on the rock mass mechanical properties.

Table 4-11. Influence on the rock mass mechanical properties of the extreme combination of input mechanical parameters (H is for the high stress level, L for the low stress level).

	E_{mH} (GPa)	ν_{mH}	E_{mL} (GPa)	ν_{mL}	ϕ_m (°)	c_m (MPa)
Comb 1	6.04	0.01	5.85	0.01	–0.23	0.49
Comb 2	–10.56	0.01	–7.57	0.00	0.67	–1.10

Table 4-12. Influence on the rock mass properties of the combinations run in 3DEC (H is for the high stress level, L for the low stress level).

	E_{mH} (GPa)	ν_{mH}	E_{mL} (GPa)	ν_{mL}	ϕ_m (°)	c_m (MPa)
Mean	–0.66	0.00	0.15	0.00	–0.13	0.45
Standard dev	3.23	0.02	2.70	0.02	0.71	1.86
Min	–10.90	–0.06	–7.56	–0.05	–1.34	–3.95
Max	6.04	0.06	5.85	0.06	2.12	3.67

4.2.3 Monte-Carlo simulations

The procedure applied for the Monte-Carlo simulations is described in Section 4.1.3.

The rock mass mechanical properties and their variation are presented in Table 4-13. The distributions were truncated such as a unique value has 95% probability to be in the range of the given distribution.

Table 4-13. Distribution of the rock mass mechanical properties (accounting for variation in fracture pattern and input parameters) of Rock Domain RFM029 parallel to σ_2.

	E_{mH} (GPa)	ν_{mH}	E_{mL} (GPa)	ν_{mL}	ϕ_m (°)	c_m (MPa)
Mean	65.45	0.24	62.55	0.25	47.99	20.87
Standard dev	3.60	0.02	4.43	0.026	3.31	6.37
Min	58.39	0.20	53.87	0.20	41.50	8.38
Max	72.51	0.29	71.23	0.30	54.48	33.36

The correlation between ϕ_m and c_m is –0.417.

Table 4-14. Distribution of the rock mass UCS (accounting for variation in fracture pattern and input parameters).

	UCS_m (MPa)
Mean	108.4
Standard dev	26.89
Min	46.13
Max	179.36

5 Simulations on the alternative 2 of DFN model

5.1 Simulations parallel to σ_1

The mechanical model was then tested for trace planes parallel to the maximal principal stress.

5.1.1 DFN geometry-induced rock mass variability

The procedure is exactly the same as described in Section 4.1.1.

The evaluated rock mass parameters, E_m and ν_m at 45 MPa and 11.3 MPa for each realisation are presented in Appendix C Tables C-1 and C-2.

The evaluated cohesion and friction angle of the rock mass for each realisation are presented in Appendix C Table C-3. These parameters were evaluated by fitting a straight line between the vertical stress at failure at both stress levels. The uniaxial compressive strength of the rock mass was calculated from the evaluated cohesion and friction angle.

A summary of the obtained distributions for $E_{m\ 45\ Mpa}$, $\nu_{m\ 45\ MPa}$, $E_{m\ 11.3\ MPa}$, $\nu_{m\ 11.3\ MPa}$, ϕ_m and c_m are summarized in Table 5-1 for Rock Domain RFM029. The parameters that are given in this table only account for the influence of the variation in the fracture pattern on the rock mass properties (as input mechanical parameters are constant).

Table 5-1. DFN geometry-induced variability in rock mass properties of Rock Domain RFM029 parallel to σ_1.

	Mean	Standard deviation	Min	Max
$E_{m\ 45\ Mpa}$ (GPa)	69.4	2.3	64.8	73.4
$\nu_{m\ 45\ MPa}$	0.24	0.004	0.23	0.25
$E_{m\ 11.3\ MPa}$ (GPa)	68.8	3.0	63.9	74.7
$\nu_{m\ 11.3\ MPa}$	0.23	0.01	0.22	0.25
ϕ_m (°)	50.1	2.2	46.9	53.9
c_m (MPa)	25.6	8.2	10.7	38.0

The correlation between the friction angle, ϕ_m, and cohesion, c_m, are 0.30227.

5.1.2 Material property influence on rock mass parameters

These simulations were run in order to assess the influence of the variation of input parameters on the rock mass mechanical parameters. This is achieved by always using the same DFN realisation while the mechanical input parameters are changed one at a time and are attributed its minimum and maximum values while all other material properties are set to their mean values. Relationships can then be established between variations in all input material parameters and their respective impact on rock mass properties.

The same confining stresses as used in Section 4.1.1 were applied on the model: 45 MPa and 11.3 MPa.

Table 5-2 presents the effect of variation for each of the input parameters on the rock mass parameters when the input parameter is given its minimum value. A positive value indicates that the rock mass mechanical parameter increases when the input parameter decreases from its mean to its minimum value.

Table 5-3 presents the effect of variation for each of the input parameters on the rock mass parameters when the input parameter is given its maximum value.

Table 5-4 presents the calculated influence on rock mass deformation modulus of 2 extreme combinations that are expected to give respectively the highest and lowest deformation modulus. The estimated influence is given in relation to the deformation modulus obtained for input parameters at their mean value.

Table 5-2. Influence on the rock mass mechanical properties of the input mechanical parameters set at their min value (H is for the high stress level, L for the low stress level).

	E_{mH} (GPa)	ν_{mH}	E_{mL} (GPa)	ν_{mL}	ϕ_m (°)	c_m (MPa)
E_i (GPa)	–4.14	0.00	–3.54	0.00	–0.37	0.89
ν_i	0.00	0.00	2.38	–0.06	–0.66	1.31
ϕ_i (°)	0.02	–0.06	0.00	0.00	–1.11	1.66
c_i (MPa)	0.02	0.00	0.00	0.00	–1.73	1.45
T_i (MPa)	0.02	0.00	0.00	0.00	–1.66	5.42
K_n (MPa/mm)	–2.68	0.00	–3.50	–0.02	–0.42	0.60
K_s (MPa/mm)	–6.58	–0.02	–5.33	0.03	–2.19	3.59
ϕ_f (°)	–0.02	0.03	–3.89	0.04	–5.61	3.91
c_f (MPa)	0.03	0.00	–1.40	0.00	–0.11	0.27

Table 5-3. Influence on the rock mass mechanical properties of the input mechanical parameters set at their max value (H is for the high stress level, L for the low stress level).

	E_{mH} (GPa)	ν_{mH}	E_{mL} (GPa)	ν_{mL}	ϕ_m (°)	c_m (MPa)
E_i (GPa)	7.17	0.00	3.36	0.00	0.03	0.14
ν_i	–0.99	0.01	1.99	0.07	0.21	–0.46
ϕ_i (°)	0.02	0.06	0.00	0.00	0.37	–0.29
c_i (MPa)	0.02	0.00	0.00	0.00	–2.82	10.97
T_i (MPa)	0.02	0.00	0.00	0.00	–0.68	1.93
K_n (MPa/mm)	2.32	0.00	1.59	0.01	–0.90	2.35
K_s (MPa/mm)	0.57	0.01	1.12	0.00	–0.11	0.64
ϕ_f (°)	0.03	–0.01	0.08	0.00	1.29	1.96
c_f (MPa)	0.06	0.00	0.06	0.00	–0.11	0.85

Table 5-4. Influence on the rock mass mechanical properties of the extreme combination of input mechanical parameters (H is for the high stress level, L for the low stress level).

	E_{mH} (GPa)	ν_{mH}	E_{mL} (GPa)	ν_{mL}	ϕ_m (°)	c_m (MPa)
Comb 1	7.17	0.00	6.58	0.01	–0.56	2.09
Comb 2	–12.29	0.01	–10.18	0.02	–2.06	3.26

Based on the calculated estimated influence of input parameter variation on the rock mass mechanical properties, specific combinations of input parameters with high and low values were chosen. These are expected to produce low and high deformation modulus or uniaxial compressive strength. 3DEC simulations were done with these combinations on DFN realisation nr 0, see Appendix C. The results of these combinations are expressed in term of mean value, standard deviation, min and max values, and are presented in Table 5-5. The mean, min and max values are given in relation to the rock mass mechanical properties for the input parameters set at their mean value.

These simulations only account for the influence of the variation of input parameters on the rock mass mechanical properties.

Table 5-5. Influence on the rock mass properties of the combinations run in 3DEC (H is for the high stress level, L for the low stress level).

	E_{mH} (GPa)	ν_{mH}	E_{mL} (GPa)	ν_{mL}	ϕ_m (°)	c_m (MPa)
Mean	–0.44	0.00	–0.31	0.00	–0.92	2.00
Standard dev	4.02	0.02	3.44	0.02	1.45	2.54
Min	–12.29	–0.06	–10.18	–0.06	–4.69	–0.46
Max	7.16	0.06	6.58	0.06	2.21	8.91

The correlation between ϕ_m and c_m is –0.62092.

5.1.3 Monte-Carlo simulations

The procedure applied for the Monte-Carlo simulations was described in Section 4.1.3.

The rock mass mechanical properties and their variation are presented in Table 5-6 and Table 5-7. The distributions were truncated such as a unique value has 95% probability to be in the range of the given distribution.

Table 5-6. Distribution of the rock mass mechanical properties (accounting for variation in fracture pattern and input parameters).

	E_{mH} (GPa)	ν_{mH}	E_{mL} (GPa)	ν_{mL}	ϕ_m (°)	c_m (MPa)
Mean	68.63	0.24	68.46	0.23	49.26	27.96
Standard dev	4.19	0.02	4.06	0.021	2.17	6.72
Min	60.42	0.20	60.50	0.19	45.00	14.79
Max	76.84	0.28	76.42	0.27	53.51	41.13

The correlation between ϕ_m and c_m is 0.11246.

Table 5-7. Distribution of the rock mass UCS (accounting for variation in fracture pattern and input parameters).

	UCS_m (MPa)
Mean	151.21
Standard dev	32.65
Min	76.38
Max	238.87

5.2 Simulations parallel to σ_2

The mechanical model was then tested for trace planes parallel to the minimal principal stress in the horizontal plane.

5.2.1 DFN geometry-induced rock mass variability

The procedure is exactly the same as described in Section 4.1.1.

The evaluated rock mass parameters, E_m and ν_m at 30.5 MPa and 8.0 MPa for each realisation are presented in Appendix D Tables D-1 and D-2.

The evaluated cohesion and friction angle of the rock mass for each realisation are presented in Appendix D Table D-3. These parameters were evaluated by fitting a straight line between the vertical stress at failure at both stress levels. The uniaxial compressive strength of the rock mass has been calculated from the evaluated cohesion and friction angle.

A summary of the obtained distributions for $E_{m\ 30.5\ Mpa}$, $\nu_{m\ 30.5\ MPa}$, $E_{m\ 8.0\ MPa}$, $\nu_{m\ 8.0\ MPa}$, ϕ_m and c_m are summarized in Table 5-8 for Rock Domain RFM029. The parameters that are given in this table only account for the influence of the variation in the fracture pattern on the rock mass properties (as input mechanical parameters are constant).

Table 5-8. DFN geometry-induced variability in rock mass properties of Rock Domain RFM029.

	Mean	Standard deviation	Min	Max
$E_{m\ 30.5\ Mpa}$ (GPa)	69.1	1.8	65.1	72.8
$\nu_{m\ 30.5\ MPa}$	0.24	0.004	0.23	0.25
$E_{m\ 8.0\ MPa}$ (GPa)	68.5	2.6	63.6	71.8
$\nu_{m\ 8.0\ MPa}$	0.23	0.009	0.22	0.25
ϕ_m (°)	50.6	2.5	45.2	54.0
c_m (MPa)	19.2	5.8	9.8	33.6

The correlation between the friction angle, ϕ_m, and cohesion, c_m, are 0.10796.

5.2.2 Material property influence on rock mass parameters

These simulations are run in order to assess the influence of the variation of input parameters on the rock mass mechanical parameters. This is achieved by using always the same DFN realisation while the mechanical input parameters are changed one at a time and are attributed its minimum and maximum values while all other material properties are set to their mean values. Relationships can then be established between variations in all input material parameters and their respective impact on rock mass properties.

The same confining stresses as used in Section 4.1.1 were applied on the model: 30.5 MPa and 8.0 MPa.

Table 5-9 presents the effect of variation for each of the input parameters on the rock mass parameters when the input parameter is given its minimum value. A positive value indicates that the rock mass mechanical parameter increases when the input parameter decreases from its mean to its minimum value.

Table 5-10 presents the effect of variation for each of the input parameters on the rock mass parameters when the input parameter is given its maximum value.

Table 5-11 presents the calculated influence on rock mass deformation modulus of 2 extreme combinations that are expected to give respectively the highest and lowest deformation modulus. The estimated influence is given in relation to the deformation modulus obtained for input parameters at their mean value.

Table 5-9. Influence on the rock mass mechanical properties of the input mechanical parameters set at their min value (H is for the high stress level, L for the low stress level).

	E_{mH} (GPa)	ν_{mH}	E_{mL} (GPa)	ν_{mL}	ϕ_m (°)	c_m (MPa)
E_i (GPa)	–3.06	0.00	–8.62	0.01	0.32	–1.55
ν_i	1.02	–0.01	–3.02	–0.05	0.32	–2.12
ϕ_i (°)	1.38	–0.07	–4.24	0.02	0.16	–0.64
c_i (MPa)	1.35	–0.01	–4.67	0.01	1.67	–7.57
T_i (MPa)	1.37	–0.01	–3.81	0.01	–0.55	0.92
K_n (MPa/mm)	–0.39	–0.01	–4.61	0.00	–1.11	3.77
K_s (MPa/mm)	–1.42	–0.02	–2.67	0.01	1.07	–0.71
ϕ_f (°)	0.97	0.01	–0.71	0.01	–2.05	0.36
c_f (MPa)	1.36	0.00	–0.41	0.00	–0.08	0.10

Table 5-10. Influence on the rock mass mechanical properties of the input mechanical parameters set at their max value (H is for the high stress level, L for the low stress level).

	E_{mH} (GPa)	ν_{mH}	E_{mL} (GPa)	ν_{mL}	ϕ_m (°)	c_m (MPa)
E_i (GPa)	5.75	–0.01	4.33	0.00	0.74	–0.61
ν_i	1.43	–0.01	–0.57	0.06	0.57	–0.12
ϕ_i (°)	1.37	0.06	0.04	0.00	0.17	0.20
c_i (MPa)	1.42	–0.01	–0.05	0.00	0.28	3.09
T_i (MPa)	1.37	–0.01	0.00	0.00	1.60	–4.17
K_n (MPa/mm)	2.31	–0.01	1.02	0.01	0.53	–2.06
K_s (MPa/mm)	1.89	0.00	0.26	0.00	–1.17	3.15
ϕ_f (°)	1.38	–0.01	0.15	0.00	2.23	–1.96
c_f (MPa)	0.56	–0.01	–0.03	0.00	–9.82	14.00

Table 5-11. Influence on the rock mass mechanical properties of the extreme combination of input mechanical parameters (H is for the high stress level, L for the low stress level).

	E_{mH} (GPa)	ν_{mH}	E_{mL} (GPa)	ν_{mL}	ϕ_m (°)	c_m (MPa)
Comb 1	7.30	0.00	6.04	0.01	–0.36	0.99
Comb 2	–6.84	0.00	–7.82	0.00	0.58	–0.24

Based on the calculated estimated influence of input parameter variation on the rock mass mechanical properties, specific combinations of input parameters with high and low values were chosen. These are expected to produce low and high deformation modulus or uniaxial compressive strength. 3DEC simulations were done with these combinations on DFN realisation nr 1. The results of these combinations are expressed in term of mean value, standard deviation, min and max values, and are presented in Table 5-12. The mean, min and max values are given in relation to the rock mass mechanical properties for the input parameters set at their mean value.

These simulations only account for the influence of the variation of input parameters on the rock mass mechanical properties.

Table 5-12. Influence on the rock mass properties of the combinations run in 3DEC (H is for the high stress level, L for the low stress level).

	E_{mH} (GPa)	ν_{mH}	E_{mL} (GPa)	ν_{mL}	ϕ_m (°)	c_m (MPa)
Mean	0.98	0.00	–1.40	0.0	–0.24	0.23
Standard dev	2.88	0.021	3.49	0.018	2.41	4.01
Min	–6.84	–0.07	–8.62	–0.05	–9.83	–7.57
Max	7.30	0.06	6.04	0.06	2.23	13.99

The correlation between ϕ_m and c_m is –0.89344.

5.2.3 Monte-Carlo simulations

The procedure applied for the Monte-Carlo simulations is described in Section 4.1.3.

The rock mass mechanical properties and their variation are presented in Table 5-13 and Table 5-14. The distributions were truncated such as a unique value has 95% probability to be in the range of the given distribution.

Table 5-13. Distribution of the rock mass mechanical properties (accounting for variation in fracture pattern and input parameters).

	E_{mH} (GPa)	ν_{mH}	E_{mL} (GPa)	ν_{mL}	ϕ_m (°)	c_m (MPa)
Mean	69.98	0.24	66.81	0.23	49.35	20.0
Standard dev	3.11	0.021	3.71	0.019	2.79	6.36
Min	63.88	0.20	59.54	0.19	43.88	7.53
Max	76.08	0.28	74.08	0.27	54.82	32.47

The correlation between ϕ_m and c_m is –0.2994.

Table 5-14. Distribution of the rock mass UCS (accounting for variation in fracture pattern and input parameters).

	UCS_m (MPa)
Mean	107.88
Standard dev	28.39
Min	42.57
Max	182.45

5.3 Summary of DFN geometry-induced rock mass variability

In figure Figure 5-1 and Figure 5-2 the results from all the 3DEC simulations on DFN-realisations for rock domain RFM029 and the two alternative DFN models are presented. The DFN alternative 2 gives a little higher deformation modulus and a slightly higher failure stress.

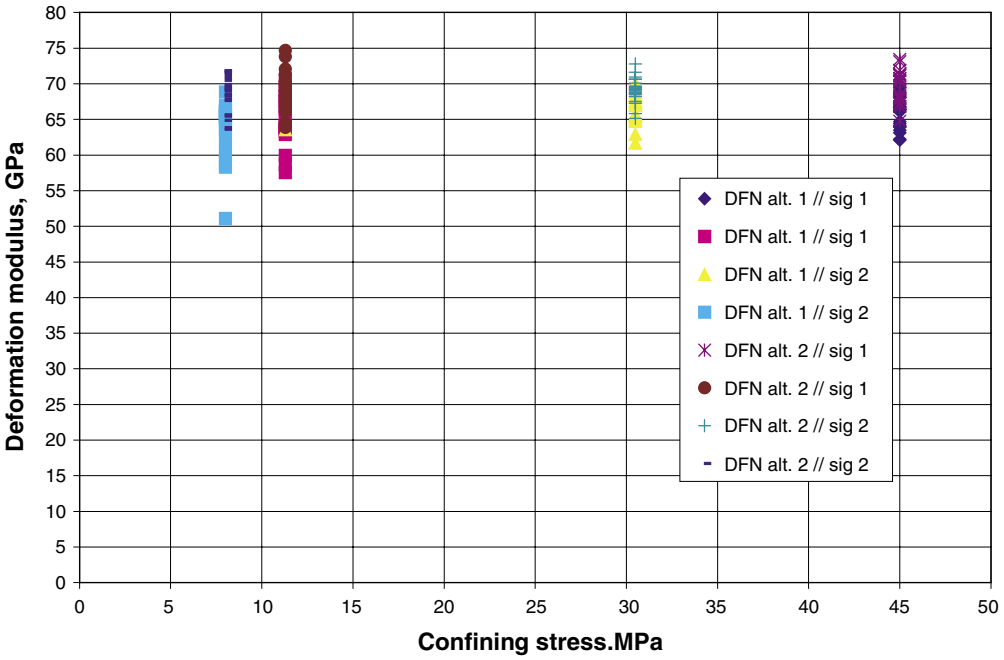

Figure 5-1. *Variation of deformation modulus with confining stress for all DFN realizations.*

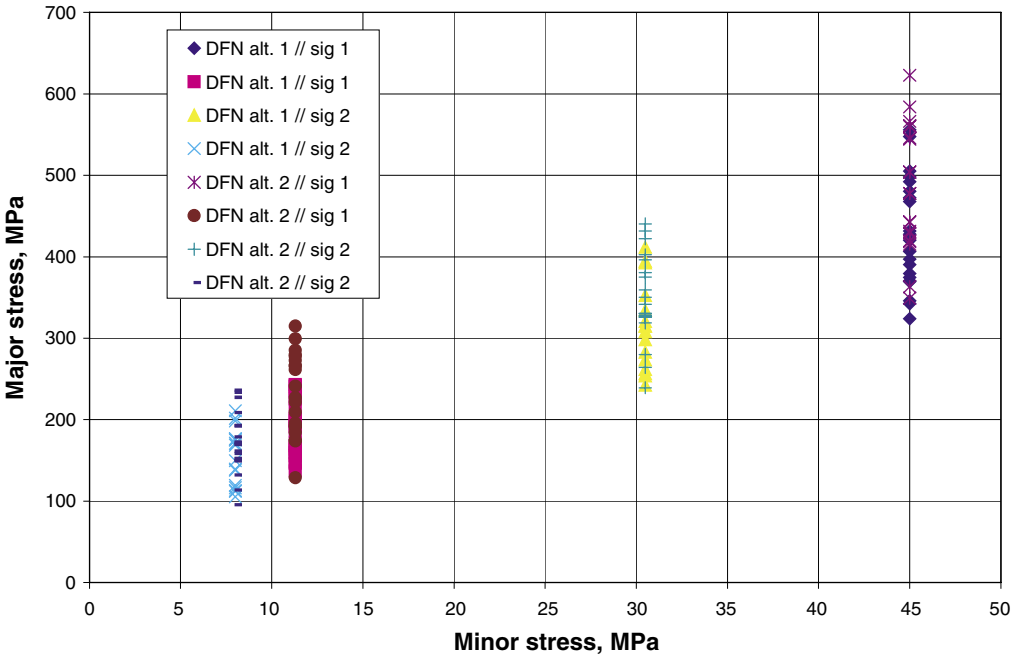

Figure 5-2. *Relationship between major and minor stress at failure in the rock mass for all DFN realizations.*

5.4 Summary of material property influence on rock mass variability

In Figure 5-3 and Figure 5-4 the results from all 3DEC simulations with different combinations of material properties on the same DFN realization. The DFN realization parallel to σ_1 is of course different from that parallel to σ_2.

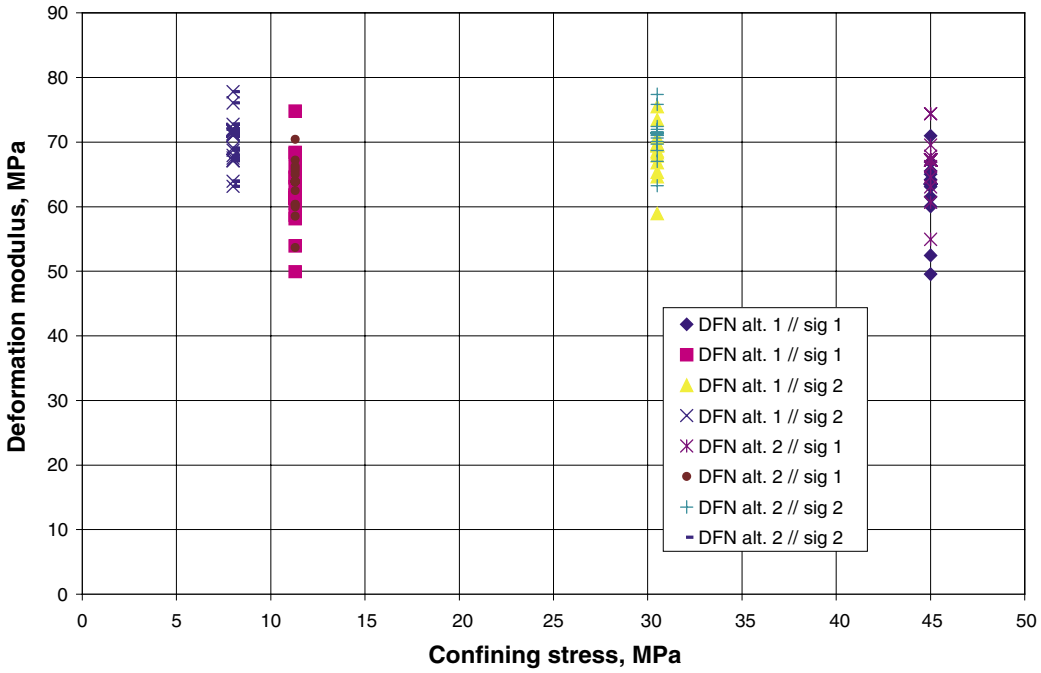

Figure 5-3. *Variation of deformation modulus with confining stress.*

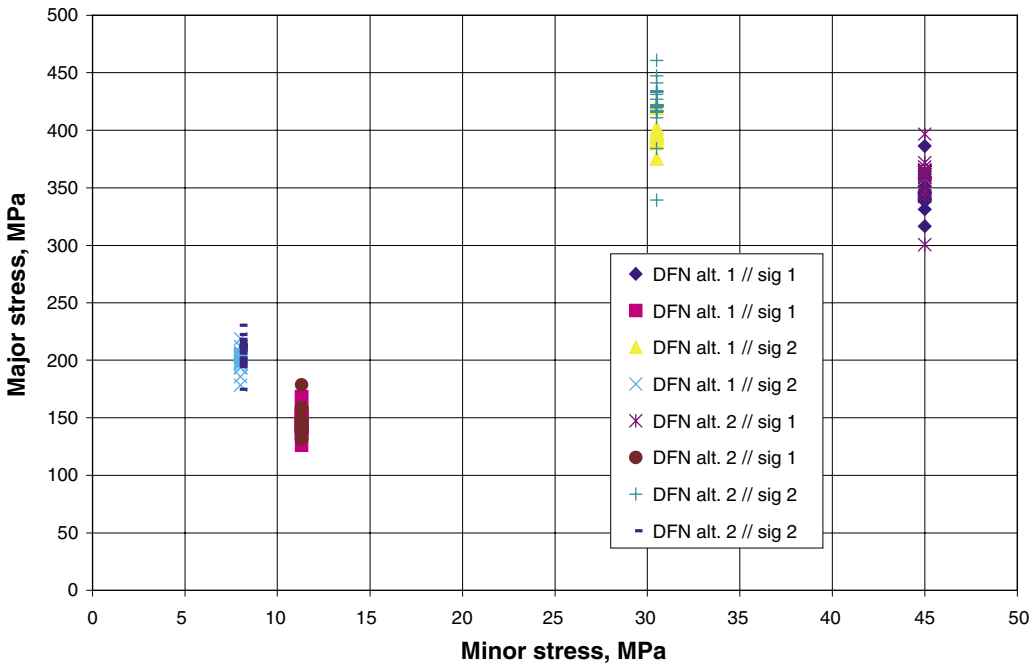

Figure 5-4. *Relationship between major and minor stress at failure in the rock mass.*

6 Simulations on the updated DFN model

6.1 Introduction

The DFN model was updated in March 2005. For this model the following analyzes were performed to see if the changes in the DFN model had any impact on the rock mass properties.

6.2 Simulations parallel to σ_1

The mechanical model was tested for trace planes parallel to the maximal principal stress.

6.2.1 DFN geometry-induced rock mass variability

The orientation of fracture sets was not changed in the updated DFN model presented in March 2005. The intensity, P_{32}, and the fracture size distribution was changed according to Table 6-1.

Table 6-1. Updated DFN model: P_{32} and size distribution for open fractures in the rock domain 29 (RFM029).

Set	P_{32} open, mean	Size distribution type	k_r	X_{r0}
NS	0.12	Power Law	2.88	0.28
NE	0.46	Power Law	3.02	0.25
NW	0.16	Power Law	2.81	0.14
EW	0.05	Power Law	2.95	0.15
SubH	0.34	Power Law	2.90	0.25

The procedure is exactly the same as described in Section 4.1.1.

The evaluated rock mass parameters, E_m and ν_m at 45 MPa and 11.3 MPa for each realisation are presented in Appendix E Tables E-1 and E-2.

The evaluated cohesion and friction angle of the rock mass for each realisation are presented in Appendix E Table E-3. These parameters were evaluated by fitting a straight line between the vertical stress at failure at both stress levels. The uniaxial compressive strength of the rock mass was calculated from the evaluated cohesion and friction angle.

A summary of the obtained distributions for $E_{m\ 45\ Mpa}$, $\nu_{m\ 45\ MPa}$, $E_{m\ 11.3\ MPa}$, $\nu_{m\ 11.3\ MPa}$, ϕ_m and c_m are summarized in Table 6-2 for Rock Domain RFM029. The parameters that are given in this table only account for the influence of the variation in the fracture pattern on the rock mass properties (as input mechanical parameters are constant).

Table 6-2. DFN geometry-induced variability in rock mass properties of Rock Domain RFM029 parallel to σ_1.

	Mean	Standard deviation	Min	Max
$E_{m\ 45\ Mpa}$ (GPa)	71.16	1.16	69.2	73.0
$\nu_{m\ 45\ MPa}$	0.24	0.01	0.23	0.27
$E_{m\ 11.3\ MPa}$ (GPa)	69.9	2.09	63.1	72.6
$\nu_{m\ 11.3\ MPa}$	0.24	0.01	0.24	0.27
ϕ_m (°)	57.7	2.1	51.9	60.7
c_m (MPa)	26.4	3.7	18.0	31.4

The correlation between the friction angle, ϕ_m, and cohesion, c_m, are –0.446.

6.3 Comparison between the different DFN-models

The DFN-geometry-induced rock mass variability from the different DFN-models is compared in Table 6-3 to Table 6-8. The DFN-model from March 2005 gives a little higher deformation modulus and higher rock mass strength as a mean value but the difference is in the range calculated with DFN-model alternative 1 and 2.

Table 6-3. Deformation modulus at high stress level.

E_{mH} (GPa)	DFN alt 1 parallel to σ_1	DFN alt 1 parallel to σ_2	DFN alt 2 parallel to σ_1	DFN alt 2 parallel to σ_2	DFN alt March 2005 parallel to σ_1
Mean	66.0	66.4	69.4	69.1	71.2
Standard dev	2.4	2.3	2.3	1.8	1.2
Min	62.1	61.7	64.8	65.1	69.2
Max	70.0	70.1	73.4	72.8	73.0

Table 6-4. Deformation modulus at low stress level.

E_{mL} (GPa)	DFN alt 1 parallel to σ_1	DFN alt 1 parallel to σ_2	DFN alt 2 parallel to σ_1	DFN alt 2 parallel to σ_2	DFN alt March 2005 parallel to σ_1
Mean	64.9	63.4	68.8	68.5	69.9
Standard dev	3.4	4.4	3.0	2.6	2.1
Min	57.5	51.1	63.9	63.6	63.1
Max	70.3	68.8	74.7	71.8	72.6

Table 6-5. Poisson's ratio at high stress level.

ν_{mH}	DFN alt 1 parallel to σ_1	DFN alt 1 parallel to σ_2	DFN alt 2 parallel to σ_1	DFN alt 2 parallel to σ_2	DFN alt March 2005 parallel to σ_1
Mean	0.24	0.24	0.24	0.24	0.24
Standard dev	0.01	0.01	0.004	0.004	0.01
Min	0.23	0.23	0.23	0.23	0.23
Max	0.25	0.25	0.25	0.25	0.27

Table 6-6. Poisson's ratio at low stress level.

ν_{mL}	DFN alt 1 parallel to σ_1	DFN alt 1 parallel to σ_2	DFN alt 2 parallel to σ_1	DFN alt 2 parallel to σ_2	DFN alt March 2005 parallel to σ_1
Mean	0.24	0.25	0.23	0.23	0.24
Standard dev	0.01	0.02	0.01	0.009	0.01
Min	0.23	0.22	0.22	0.22	0.24
Max	0.27	0.31	0.25	0.25	0.27

Table 6-7. Friction angle of the rock mass.

ϕ_m (°)	DFN alt 1 parallel to σ_1	DFN alt 1 parallel to σ_2	DFN alt 2 parallel to σ_1	DFN alt 2 parallel to σ_2	DFN alt March 2005 parallel to σ_1
Mean	48.4	48.3	50.1	50.6	52.1
Standard dev	3.1	3.8	2.2	2.5	2.4
Min	42.6	40.1	46.9	45.2	45.5
Max	53.6	54.7	53.9	54.1	55.5

Table 6-8. Cohesion of the rock mass.

c_m (MPa)	DFN alt 1 parallel to σ_1	DFN alt 1 parallel to σ_2	DFN alt 2 parallel to σ_1	DFN alt 2 parallel to σ_2	DFN alt March 2005 parallel to σ_1
Mean	21.0	18.8	25.6	19.2	31.1
Standard dev	4.8	7.5	8.2	5.8	4.4
Min	13.8	10.2	10.8	8.8	21.3
Max	28.6	40.5	38.0	33.6	37.1
Correlation between ϕ_m and c_m	0.0489	–0.44	0.3027	0.10796	–0.447

7 Discussions and conclusions

The data uncertainty and variability was studied in two steps, first by analysing the influence of the fracture pattern, and then by studying the influence of the variation of the input parameters. Their combined effect is analysed by means of Monte-Carlo simulations.

The resulting rock mass mechanical properties and their variation are presented in Table 7-1 to Table 7-7 for the two alternative DFN models and in sections parallel to the minimum and maximum horizontal stresses (σ_2 and σ_1).

Stochastic variability in fracture properties among fractures in DFN realisations have not been examined, because of limitations in 3DEC. Instead, all fractures within a DFN realisation have been assigned the same values: either their minimum, mean or maximum parameter values. This will probably overestimated the effect of the input parameter variability on rock mass properties.

The DFN-induced variability component is only evaluated for a limited number of realisations (20).

The influences of input parameters on rock mass properties have only been examined for one DFN realisation in the rock domain RFM029.

Before the design values of the material properties of the rock mass are determined the results of the theoretical approach shall be harmonized with the empirical approach.

Table 7-1. Deformation modulus at high stress level.

E_{mH} (GPa)	DFN alt 1 parallel to σ_1	DFN alt 1 parallel to σ_2	DFN alt 2 parallel to σ_1	DFN alt 2 parallel to σ_2
Mean	64.9	65.5	68.6	70.0
Standard dev	4.5	3.6	4.2	3.1
Min	56.1	58.4	60.4	63.9
Max	73.8	72.5	76.8	76.1

Table 7-2. Deformation modulus at low stress level.

E_{mL} (GPa)	DFN alt 1 parallel to σ_1	DFN alt 1 parallel to σ_2	DFN alt 2 parallel to σ_1	DFN alt 2 parallel to σ_2
Mean	68.0	62.56	68.5	66.8
Standard dev	5.6	4.4	4.1	3.7
Min	57.0	53.9	60.5	59.5
Max	79.1	71.2	76.4	74.1

Table 7-3. Poisson's ratio at high stress level.

ν_{mH}	DFN alt 1 parallel to σ_1	DFN alt 1 parallel to σ_2	DFN alt 2 parallel to σ_1	DFN alt 2 parallel to σ_2
Mean	0.25	0.24	0.24	0.24
Standard dev	0.02	0.02	0.02	0.021
Min	0.21	0.20	0.20	0.20
Max	0.29	0.29	0.28	0.28

Table 7-4. Poisson's ratio at low stress level.

ν_{mL}	DFN alt 1 parallel to σ_1	DFN alt 1 parallel to σ_2	DFN alt 2 parallel to σ_1	DFN alt 2 parallel to σ_2
Mean	0.22	0.25	0.23	0.23
Standard dev	0.02	0.026	0.021	0.019
Min	0.18	0.20	0.19	0.19
Max	0.26	0.30	0.27	0.27

Table 7-5. Friction angle of the rock mass.

ϕ_m (°)	DFN alt 1 parallel to σ_1	DFN alt 1 parallel to σ_2	DFN alt 2 parallel to σ_1	DFN alt 2 parallel to σ_2
Mean	48.5	48.0	49.3	49.4
Standard dev	2.7	3.3	2.2	2.8
Min	43.3	41.5	45.0	43.9
Max	53.7	54.5	53.5	54.8

Table 7-6. Cohesion of the rock mass.

c_m (MPa)	DFN alt 1 parallel to σ_1	DFN alt 1 parallel to σ_2	DFN alt 2 parallel to σ_1	DFN alt 2 parallel to σ_2
Mean	20.8	20.9	28.0	20.0
Standard dev	4.0	6.4	6.7	6.4
Min	12.9	8.4	14.8	7.5
Max	28.7	33.4	41.1	32.5
Correlation between ϕ_m and c_m	0.043	–0.417	0.11246	–0.2994

Table 7-7. The uniaxial compressive strength of the rock mass, UCS_m.

UCS_m (MPa)	DFN alt 1 parallel to σ_1	DFN alt 1 parallel to σ_2	DFN alt 2 parallel to σ_1	DFN alt 2 parallel to σ_2
Mean	110.3	108.4	151.2	107.9
Standard dev	19.70	26.9	32.7	28.4
Min	64.2	46.1	76.4	42.6
Max	165.4	179.4	238.9	182.5

8 References

Lanaro F, Fredriksson A, 2005. Forsmark v. 1.2. Rock Mechanics Model. Summary of the primary data, in progress.

LaPointe P R, Olofsson I, Hermanson J, 2005. Statistical model of fractures and deformation zones for Forsmark. Preliminary site description Forsmark area – version 1.2. SKB R-05-26. Svensk Kärnbränslehantering AB.

Olofsson I, Fredriksson F, 2005. Strategy for a numerical Rock Mechanics Site Descriptive Model. Further development of the theoretical/numerical approach. SKB R-05-43. Svensk Kärnbränslehantering AB.

Appendix A

Table A-1. Poisson's ratio, deformation modulus and vertical stress at failure for all DFN realisations, high stress level (45 MPa).

DFN realisation	Poisson's ratio, ν_m	Deformation modulus, E_m, GPa	Vertical stress at failure, σ_{vf}, MPa
0	0.24	63.48	342.59
1	0.25	70.01	505.09
2	0.24	66.64	420.45
3	0.23	64.71	547.51
4	0.24	63.92	374.48
5	0.24	67.28	379.55
6	0.24	66.64	492.27
7	0.25	62.21	370.20
8	0.24	69.51	555.78
9	0.25	63.96	369.60
10	0.24	64.41	467.71
11	0.24	66.79	406.77
12	0.24	68.20	480.32
13	0.25	66.08	323.88
14	0.24	62.07	390.49
15	0.24	68.41	497.97
16	0.24	64.15	397.16
17	0.25	63.12	431.55
18	0.23	66.19	472.49
19	0.24	68.55	345.77
20	0.24	68.70	427.66
Mean	0.24	65.95	428.54
Standard dev	0.005	2.41	67.68
Min	0.23	62.07	323.88
Max	0.25	70.01	555.78

Table A-2. Poisson's ratio, deformation modulus and vertical stress at failure for all DFN realisations, low stress level (11.3 MPa).

DFN realisation	Poisson's ratio, ν_m	Deformation modulus, E_m, GPa	Vertical stress at failure, σ_{vf}, MPa
0	0.27	58.65	146.42
1	0.24	68.28	240.77
2	0.27	63.66	198.97
3	0.23	66.54	235.17
4	0.26	57.54	147.79
5	0.26	63.44	155.66
6	0.24	63.91	225.66
7	0.23	59.94	167.96
8	0.24	69.54	243.12
9	0.23	67.95	191.41
10	0.24	62.87	226.60
11	0.24	70.28	164.21
12	0.25	66.95	211.04
13	0.23	68.63	136.89
14	0.24	63.27	163.72
15	0.24	67.62	242.15
16	0.23	66.29	159.37
17	0.24	63.90	185.96
18	0.23	65.22	194.59
19	0.26	64.07	170.91
20	0.26	63.57	201.06
Mean	0.24	64.86	190.93
Standard dev	0.01	3.42	34.83
Min	0.23	57.54	136.89
Max	0.27	70.28	243.12

Table A-3. Friction angle, cohesion and uniaxial compressive strength for all DFN realisations.

DFN realisation	Friction angle, ϕ_m	Cohesion, c_m, MPa	Uniaxial compressive strength, MPa
0	44.97	16.71	80.64
1	50.70	27.16	152.14
2	47.38	24.32	124.71
3	53.63	21.42	130.44
4	47.83	13.84	71.78
5	47.59	15.63	80.59
6	50.86	24.22	136.26
7	45.59	20.44	100.15
8	53.65	22.70	138.28
9	42.99	28.63	131.66
10	49.00	27.25	145.75
11	49.12	15.45	82.88
12	51.04	21.36	120.75
13	43.99	15.75	74.19
14	47.84	16.90	87.68
15	50.10	28.38	156.37
16	48.74	14.99	79.64
17	49.35	19.19	103.61
18	51.60	17.66	101.41
19	42.60	24.65	112.28
20	47.82	24.12	125.08
Mean	48.40	20.99	111.25
Standard dev	3.11	4.81	27.34
Min	42.60	13.84	71.78
Max	53.65	28.63	156.37

The correlation between the friction angle, ϕ_m, and cohesion, c_m, are 0.0489.

Appendix B

Table B-1. Poisson's ratio, deformation modulus and vertical stress at failure for all DFN realisations, high stress level (30.5 MPa).

DFN realisation	Poisson's ratio, ν_m	Deformation modulus, E_m, GPa	Vertical stress at failure, σ_{vf}, MPa
1	0.24	69.48	394.77
2	0.24	67.15	253.73
3	0.24	67.46	283.01
4	0.23	65.70	320.92
5	0.24	68.76	298.59
8	0.24	64.73	273.64
9	0.24	67.56	411.89
10	0.23	65.40	334.51
11	0.25	65.67	352.56
12	0.24	66.99	314.95
13	0.24	68.23	308.36
14	0.25	61.68	315.03
17	0.24	62.92	261.89
18	0.24	65.08	242.30
19	0.24	70.10	392.73
20	0.24	65.53	256.43
Mean	0.24	66.40	313.46
Standard dev	0.005	2.27	52.86
Min	0.23	61.68	242.30
Max	0.25	70.10	411.89

Table B-2. Poisson's ratio, deformation modulus and vertical stress at failure for all DFN realisations, low stress level (8.0 MPa).

DFN realisation	Poisson's ratio, ν_m	Deformation modulus, E_m, GPa	Vertical stress at failure, σ_{vf}, MPa
1	0.25	64.95	198.38
2	0.23	68.84	105.26
3	0.25	65.24	116.57
4	0.27	58.96	176.73
5	0.25	66.33	138.09
8	0.23	65.99	119.44
9	0.25	65.59	201.73
10	0.22	66.15	175.82
11	0.25	65.32	175.05
12	0.25	66.95	211.04
13	0.28	58.27	149.67
14	0.31	51.08	168.73
17	0.22	62.08	111.94
18	0.27	60.39	113.19
19	0.26	64.07	170.91
20	0.23	63.63	139.28
Mean	0.25	63.36	154.49
Standard dev	0.02	4.39	34.96
Min	0.22	51.08	105.26
Max	0.31	68.84	211.04

Table B-3. Friction angle, cohesion and uniaxial compressive strength for all DFN realisations.

DFN realisation	Friction angle, ϕ_m, °	Cohesion, c_m, MPa	Uniaxial compressive strength, MPa
1	52.60	21.76	128.55
2	47.46	10.21	52.47
3	49.63	10.55	57.39
4	46.89	24.78	125.46
5	48.95	15.17	81.02
8	48.19	12.34	64.61
9	53.76	20.78	127.01
10	48.73	22.48	119.40
11	50.81	19.93	111.94
12	40.09	40.51	174.09
13	48.73	17.56	93.25
14	47.17	22.89	116.71
17	47.65	11.35	58.62
18	44.68	14.04	67.28
19	54.67	14.66	92.04
20	42.67	21.39	97.63
Mean	48.29	18.77	97.97
Standard dev	3.78	7.53	33.66
Min	40.09	10.21	52.47
Max	54.67	40.51	174.09

The correlation between ϕ_m and c_m is –0.44.

Appendix C

Table C-2. Poisson's ratio, deformation modulus and vertical stress at failure for all DFN realisations, high stress level (45 MPa).

DFN realisation	Poisson's ratio, ν_m	Deformation modulus, E_m, GPa	Vertical stress at failure, σ_{vf}, MPa
0	0.24	67.23	363.21
1	0.24	70.76	504.04
2	0.23	71.22	583.91
3	0.24	67.22	429.12
4	0.24	66.79	544.37
5	0.24	71.41	477.92
6	0.24	70.45	566.30
7	0.23	67.28	477.83
8	0.25	68.44	349.25
9	0.24	67.89	419.75
10	0.24	70.65	622.79
11	0.24	68.26	443.11
12	0.24	68.06	431.02
13	0.25	69.23	418.70
14	0.24	73.09	560.29
15	0.24	70.27	442.03
16	0.23	64.77	415.50
17	0.24	71.10	560.32
18	0.23	67.90	561.13
19	0.24	71.88	504.11
20	0.24	73.43	545.77
Mean	0.24	69.40	486.69
Standard dev	0.004	2.26	76.45
Min	0.23	64.77	349.25
Max	0.25	73.43	622.79

Table C-3. Poisson's ratio, deformation modulus and vertical stress at failure for all DFN realisations, low stress level (11.3 MPa).

DFN realisation	Poisson's ratio, ν_m	Deformation modulus, E_m, GPa	Vertical stress at failure, σ_{vf}, MPa
0	0.23	63.86	140.53
1	0.24	69.80	266.67
2	0.23	71.27	266.04
3	0.24	64.45	209.43
4	0.24	66.47	226.82
5	0.25	69.91	221.68
6	0.25	69.05	285.29
7	0.24	66.12	261.48
8	0.23	67.45	128.91
9	0.23	67.67	195.73
10	0.24	70.17	314.92
11	0.23	66.81	191.49
12	0.23	68.30	184.33
13	0.23	72.04	174.56
14	0.23	73.80	279.60
15	0.23	71.32	192.24
16	0.22	64.02	173.88
17	0.23	70.32	272.76
18	0.23	68.23	299.40
19	0.22	69.00	241.21
20	0.24	74.66	277.75
Mean	0.23	68.80	228.80
Standard dev	0.01	2.96	53.15
Min	0.22	63.86	128.91
Max	0.25	74.66	314.92

Table C-4. Friction angle, cohesion and uniaxial compressive strength for all DFN realisations.

DFN realisation	Friction angle, ϕ_m	Cohesion, c_m, MPa	Uniaxial compressive strength, MPa
0	47.49	12.81	65.86
1	48.71	35.24	187.08
2	53.93	25.96	159.45
3	47.22	26.59	135.77
4	53.91	19.60	120.34
5	50.13	24.62	135.76
6	51.80	33.08	191.06
7	46.92	37.28	188.94
8	47.28	10.76	55.03
9	47.60	23.39	120.61
10	53.39	35.02	211.69
11	49.80	19.60	107.12
12	49.43	18.78	101.61
13	49.24	17.22	92.70
14	51.78	32.13	185.48
15	49.66	19.92	108.48
16	49.04	17.34	92.86
17	52.20	30.18	176.34
18	50.52	37.97	211.64
19	50.60	27.40	153.06
20	50.95	33.31	187.88
Mean	50.08	25.63	142.32
Standard dev	2.18	8.17	47.50
Min	46.92	10.76	55.03
Max	53.93	37.97	211.69

The correlation between ϕ_m and c_m is 0.30227.

Appendix D

Table D-1. Poisson's ratio, deformation modulus and vertical stress at failure for all DFN realisations, high stress level (30.5 MPa).

DFN realisation	Poisson's ratio, ν_m	Deformation modulus, E_m, GPa	Vertical stress at failure, σ_{vf}, MPa
1	0.24	70.08	422.11
2	0.25	67.24	350.26
3	0.24	69.39	330.26
4	0.24	68.45	325.83
5	0.24	69.49	327.74
6	0.24	68.87	328.31
7	0.25	65.12	264.26
8	0.25	68.56	341.67
9	0.24	70.91	380.64
10	0.24	67.54	359.24
11	0.23	68.17	318.77
12	0.24	69.08	326.11
13	0.23	69.17	431.55
14	0.24	71.61	440.26
15	0.24	70.64	239.22
16	0.24	65.82	279.95
17	0.24	72.76	402.32
18	0.24	69.66	330.57
19	0.24	70.61	396.37
20	0.24	68.71	374.96
Mean	0.24	69.09	348.52
Standard dev	0.004	1.83	53.78
Min	0.23	65.12	239.22
Max	0.25	72.76	440.26

Table D-2. Poisson's ratio, deformation modulus and vertical stress at failure for all DFN realisations, low stress level (8.0 MPa).

DFN realisation	Poisson's ratio, ν_m	Deformation modulus, E_m, GPa	Vertical stress at failure, σ_{vf}, MPa
1	0.24	71.75	208.78
2	0.23	67.87	178.94
3	0.24	71.29	152.28
4	0.23	65.46	149.64
5	0.22	64.88	170.00
6	0.25	68.95	172.43
7	0.24	65.65	132.10
8	0.25	69.86	158.45
9	0.22	69.22	171.56
10	0.24	67.65	149.28
11	0.22	63.62	161.35
12	0.23	71.82	151.51
13	0.22	69.32	227.46
14	0.23	71.61	233.64
15	0.23	63.84	95.42
16	0.23	68.46	113.51
17	0.23	70.88	192.31
18	0.24	70.46	169.35
19	0.23	69.65	236.25
20	0.24	68.34	192.78
Mean	0.23	68.53	170.85
Standard dev	0.009	2.62	37.16
Min	0.22	63.62	95.42
Max	0.25	71.82	236.25

Table D-3. Friction angle, cohesion and uniaxial compressive strength for all DFN realisations.

DFN realisation	Friction angle, ϕ_m	Cohesion, c_m, MPa	Uniaxial compressive strength, MPa
1	54.02	21.59	132.93
2	50.16	21.39	118.03
3	50.85	15.82	89.00
4	50.67	15.54	86.99
5	48.62	21.51	113.91
6	48.39	22.23	117.01
7	45.16	17.56	85.11
8	51.38	16.35	93.31
9	53.68	15.95	97.22
10	53.75	12.21	74.63
11	48.58	19.92	105.38
12	50.51	16.05	89.43
13	53.26	25.72	154.89
14	53.47	26.43	160.18
15	46.84	8.76	44.30
16	49.63	9.99	54.33
17	53.75	19.25	117.64
18	49.03	20.93	112.03
19	48.90	33.61	179.32
20	51.27	22.49	128.00
Mean	50.60	19.16	107.68
Standard dev	2.52	5.81	33.57
Min	45.16	8.76	44.30
Max	54.02	33.61	179.32

The correlation between ϕ_m and c_m is 0.10796.

Appendix E

Table E-1. Poisson's ratio, deformation modulus and vertical stress at failure for all DFN realisations, high stress level (45 MPa).

DFN realisation	Poisson's ratio, ν_m	Deformation modulus, E_m, GPa	Vertical stress at failure, σ_{vf}, MPa
1	0.24	72.73	505.76
2	0.24	70.90	549.14
3	0.24	72.92	625.32
4	0.23	71.01	646.27
5	0.23	72.03	658.97
6	0.24	71.21	582.61
7	0.24	70.19	492.01
8	0.23	70.43	613.56
10	0.23	69.35	551.37
11	0.24	69.87	434.70
12	0.24	71.18	595.30
13	0.24	70.13	556.77
14	0.24	70.47	558.29
15	0.24	71.74	554.32
16	0.24	72.97	595.55
17	0.27	69.20	579.43
18	0.24	72.65	531.67
19	0.24	71.30	593.89
20	0.24	71.76	580.41
Mean	0.24	71.16	568.70
Standard dev	0.01	1.16	53.85
Min	0.23	69.20	434.70
Max	0.27	72.97	658.97

Table E-2. Poisson's ratio, deformation modulus and vertical stress at failure for all DFN realisations, low stress level (13.5 MPa).

DFN realisation	Poisson's ratio, ν_m	Deformation modulus, E_m, GPa	Vertical stress at failure, σ_{vf}, MPa
1	0.26	69.62	263.26
2	0.24	70.44	263.29
3	0.24	72.63	319.65
4	0.24	70.49	296.21
5	0.24	71.83	314.04
6	0.24	70.48	272.92
7	0.24	68.55	235.85
8	0.24	70.46	310.81
10	0.24	67.37	267.93
11	0.27	63.10	233.20
12	0.24	70.79	282.93
13	0.24	68.97	287.76
14	0.25	69.05	238.30
15	0.24	71.34	257.72
16	0.24	72.13	283.93
17	0.24	69.93	303.34
18	0.25	71.09	284.07
19	0.24	70.20	278.34
20	0.24	69.25	304.57
Mean	0.24	69.88	278.85
Standard dev	0.01	2.09	26.14
Min	0.24	63.10	233.20
Max	0.27	72.63	319.65

Table E-3. Friction angle, cohesion and uniaxial compressive strength for all DFN realisations.

DFN realisation	Friction angle, ϕ_m	Cohesion, c_m, MPa	Uniaxial compressive strength, MPa
1	49.11	33.91	181.95
2	52.10	28.75	167.44
3	53.26	36.05	217.16
4	55.52	27.74	178.83
5	55.28	31.00	198.38
6	53.49	27.89	169.08
7	50.13	27.20	149.96
8	53.10	34.91	209.29
10	51.95	29.81	172.89
11	45.52	33.87	165.63
12	53.63	29.26	178.19
13	51.02	34.96	197.56
14	54.04	21.26	131.00
15	52.74	26.67	158.27
16	53.59	29.50	179.44
17	51.48	36.82	210.76
18	49.50	37.09	201.05
19	53.81	28.19	172.53
20	51.47	37.06	212.08
Mean	52.14	31.16	181.66
Standard dev	2.39	4.40	23.12
Min	45.52	21.26	131.00
Max	55.52	37.09	217.16

The correlation between ϕ_m and c_m is –0.447.